

Review

Manuscript for submission to *Advanced Healthcare Materials*

Integrin Clustering Matters: A Review of Biomaterials Functionalized with Multivalent Integrin-Binding Ligands to Improve Cell Adhesion, Migration, Differentiation, Angiogenesis, and Biomedical Device Integration

Fatemeh Karimi^{1,2}, Andrea J O'Connor¹, Greg Qiao^{2*}, Daniel E Heath^{1*}

¹ School of Chemical and Biomedical Engineering, Particulate Fluids Processing Centre, University of Melbourne, Parkville VIC 3010, Australia

² Polymer Science Group, Department of Chemical Engineering, Particulate Fluid Processing Centre, University of Melbourne, Parkville VIC 3010, Australia

* Co-corresponding Authors

Daniel E Heath

Tel: +61 3 8344 2579

Fax: +61 3 8344 4153

Email: daniel.heath@unimelb.edu.au

Greg Qiao

This is the author manuscript accepted for publication and has undergone full peer review but has not been through the copyediting, typesetting, pagination and proofreading process, which may lead to differences between this version and the [Version of Record](#). Please cite this article as [doi: 10.1002/adhm.201701324](https://doi.org/10.1002/adhm.201701324).

This article is protected by copyright. All rights reserved.

Tel: +61 3 8344 8665
Fax: +61 3 8344 4153
Email: gregghq@unimelb.edu.au

Abstract

Material systems that exhibit tailored interactions with cells are a cornerstone of biomaterial and tissue engineering technologies. One method of achieving these tailored interactions is to biofunctionalize materials with peptide ligands that bind integrin receptors present on the cell surface. However, cell biology research has illustrated that both integrin binding and integrin clustering is required to achieve a full adhesion response. This biophysical knowledge has motivated researchers to develop material systems biofunctionalized with nano-scale clusters of ligands that promote both integrin occupancy and clustering of the receptors. These materials have improved a wide variety of biological interactions in vitro including cell adhesion, proliferation, migration speed, gene expression, and stem cell differentiation; and improved in vivo outcomes including increased angiogenesis, tissue healing, and biomedical device integration. This review first introduces the techniques that enable fabrication of these nano-patterned materials, describes the improved biological effects that have been achieved, and lastly discusses the current limitations of the technology and where future advances may occur. Although this technology is still in its nascency, it will undoubtedly play an important role in the future development of biomaterials and tissue engineering scaffolds for both in vitro and in vivo applications.

Keywords: nanopatterning, multivalent ligands, focal adhesion, cell signalling, biomaterials

1. Introduction

Developing material systems that direct specific cellular behaviours is a major goal of biomaterials scientists and tissue engineers. Not only are these materials potentially useful as medical devices and tissue scaffolds, but they also generate well-controlled platforms for the study of fundamental biological phenomena. For instance, basic material properties of cell culture substrates such as chemical composition, stiffness, and topography have been shown to influence a wide variety of adherent cell behaviours including adhesion, migration, gene expression, and differentiation.^[1-4] One of the most powerful and promising strategies for generating advanced biomaterials with tailored cellular interactions is biofunctionalization, a process by which biologically active components are incorporated into the materials of interest. If appropriately tethered, these components retain their bioactivity, interact with high specificity with receptors located on the cell surface, and drive specific cellular behaviours.^[5-7]

Integrins are the major family of cell receptors responsible for adhesion between cells and their external environment, the extracellular matrix (ECM).^[8-11] In addition to anchoring cell to their surroundings, integrins also connect internally to the cell's cytoskeleton. Thus, integrin binding is critical to a variety of cellular activities such as adhesion, spreading, cytoskeletal organization, mechanotransduction, and migration. Additionally, integrin binding is a necessary step in multiple intracellular signalling pathways.^[8,9] For these reasons, integrin receptors are a common target in order to obtain adhesion of specific cell types to a material and to promote cell-specific functions.

In vivo, integrins bind with high specificity to proteins in the ECM such as collagen, fibronectin, and laminin. However, immobilization of the full protein onto a biomaterial is not always necessary in order to elicit an integrin binding event. Instead, recombinant protein fragments or short polypeptide ligands are often sufficient to result in integrin binding. These protein fragments and peptides are often easier to incorporate into materials whilst retaining their bioactivity. One of the most common recombinant protein fragments utilized in biomaterials work is the 7th to 10th repeat of the fibronectin type III domain (FNIII₇₋₁₀) that contains an RGD binding site on the 10th repeat and a synergy group on the 9th repeat.^[10, 12] Additionally, many short polypeptide ligands have been identified including the collagen-mimic peptide GEOGER, the IKVAV peptide derived from laminin, and the TPS peptide discovered through phage display.^[7, 13, 14] However, the most common ligand used to engage integrin receptors is the RGD peptide that is found in fibronectin and vitronectin.^[6, 15, 16] A detailed description of the variety of integrin-binding ligands that have been used in biomaterial applications is beyond the scope of this contribution. However, several high quality reviews are available.^[8, 17-19]

A common strategy for generating integrin-binding biomaterials is to synthesize a non-fouling material that is decorated with the ligand of interest. Non-fouling materials include polyethylene glycol (PEG); zwitterionic materials, such as sulfobetaine, carboxybetaine, and phosphorylcholine; and biologically derived materials such as alginate.^[20-24] When exposed to a physiological environment, these materials develop a hydration layer with water molecules present in the aqueous phase, and this hydration layer prevents adsorption of biomolecules and subsequent cell adhesion to the material surface.^[20] Thus when these materials are functionalized with integrin-binding molecules and then seeded with cells expressing the complementary receptor, researchers often observe improved cell adhesion and spreading that

occurs due to specific interactions between integrin receptors and the peptide ligands. While there are many instances in the literature where full ECM components such as collagen, elastin, or hyaluronic acid are used to fabricate healthcare devices, it is often advantageous to work with these biofunctionalized synthetics. Synthetics are often desirable as they usually possess improved reproducibility between batches, possess more easily tuned mechanical properties, and are often less expensive to produce at industrial scale. Additionally, functionalizing non-fouling materials with specific integrin binding ligands leads to very well controlled and tailorable cell-material interactions that may not be possible when using the full biomolecule. For instance, cellular behaviours such as adhesion and spreading respond significantly to the *global surface density* of ligand. Messina and Hubbell illustrated that the adhesion and spreading of human foreskin fibroblasts increased with increasing surface density of an RGD peptide on minimally adhesive glass substrates up to a saturation point of 1 fmol/cm^2 , with no further increase up to 10^4 fmol/cm^2 .^[25]

However, the presence of the cell adhesive ligands on a material surface alone is not sufficient to elicit a full cell adhesion response that includes recruitment of key intracellular proteins and initiation of intracellular signaling as observed through tyrosine phosphorylation (described in more detail in section 2). Miyamoto et al. illustrated that in addition to the global ligand surface density, the nano-scale distribution of these ligands on the surface – or the *local ligand density* – is also critically important.^[26] The researchers illustrated that a full cell adhesion response requires two criteria to be fulfilled: 1) the integrin receptors must be occupied by a ligand and 2) the integrin receptors must be clustered within the cell membrane. Additionally, this research illustrated that the nano-scale clustering of ligands on the material surface aided in achieving both of these criteria.^[26] Indeed, many ECM

components present multimeric ligands including polymerized fibronectin and tenascin-C.^[27, 28]

However, before this contribution by Miyamoto, the biomaterials community had not appreciated the significance of multivalency in ligand presentation. This seminal discovery by Miyamoto et al.,^[26] spurred on the development of many cell culture surfaces that enable independent control over both the global and local ligand surface density. It is these technologies, along with the improved biological responses, that are the focus of this review. In section 2 of this article, we discuss the importance of integrin clustering and the biophysical mechanisms that underpin these technologies; in section 3 we thoroughly review the fabrication techniques that have been developed in order to generate such advanced cell culture surfaces and describe the biological interaction with these materials; in section 4 we describe the overarching biomaterials design principles that we can learn from these studies; and in section 5 propose potential future impacts that this technology may have in the fields of biomaterials science and tissue engineering.

2. Why Integrin Clustering is Critical

Integrins are the main family of cell-surface receptors that mediate adhesion between the cell and the ECM. 24 distinct integrin receptors can be found in humans. All integrin receptors span the cell membrane, with a large extracellular domain and a short intracellular domain. The extracellular portion of the integrin binds specific amino acid sequences present in the cells' environment while the intracellular domain usually acts as a link to the cell's cytoskeleton (**Figure 1A**).^[29-32]

Each receptor is composed of two non-covalently associated glycoproteins, the α and the β subunit. In mammals, 18 distinct α subunits and 8 distinct β subunits have been identified.

Through different combinations of these subunits the 24 integrin receptors found in humans can be formed. There is great diversity in both the locations of the integrin receptors in the human body and their binding capacity. Some integrin receptors such as $\alpha_5\beta_1$ are present on most adherent cell types as they have a common function of binding the abundant ECM protein fibronectin.^[12, 33] Other integrin receptors are only present on specific cell types and have much more specialized functions such as the $\alpha_{IIb}\beta_3$ receptor that is found on platelets, interacts with biomolecules such as fibrinogen and von Willibrand factor, and plays a critical role in platelet activation and blood clotting.^[34]

Integrin receptors are not stationary within the cell membrane. Due to the fluid-like nature of the lipid bilayer the receptors can move in relation to one another. In fact, this movement within the cell membrane is critical to their function. After the initial integrin-ligand binding event, additional integrin receptors and a myriad of other cytosolic proteins will be recruited to the adhesion site in order to form *adhesion complexes*. These complexes are dynamic multi-protein structures that can range in size from nascent adhesions (<250nm) to focal adhesions (~500nm) to streak-like fibrillary adhesions (>5 μ m).^[35] These complexes can contain upwards of 80 different types of proteins. Some proteins present in these complexes such as talin and vinculin act in recruitment of additional components, stabilization of the complex, and connection to the cytoskeleton; others are adaptor proteins such as paxillin, tensin, and p130cas; and others still are signalling molecules, such as focal adhesion kinase (FAK) and Src-family kinases.^[12, 35-39] A detailed description of the formation, maturation, and signalling mechanisms of these complexes is beyond the scope of this article; however, many excellent reviews on these subjects can be found here.^[39-41]

These complexes play a critical role in many signalling pathways that drive a wide variety of cellular functions. Since integrin receptors act as the link between the extracellular environment and the cytoskeleton, it seems natural that these complexes act as nexus for events relating to cell adhesion, morphology, and migration. Indeed, many studies have illustrated that integrins and the complexes they form are critical mediators of these cellular behaviours.^[29, 37, 38, 42, 43] However, integrins also play a role in the regulation of many other cellular functions. The most dramatic example is anchorage dependent cells that must be attached to a substrate via integrin interactions in order to survive. This phenomenon was clearly shown with endothelial cells via two mechanisms: 1) when endothelial cells were detached from a surface through the addition of the soluble RGD peptide the cells entered apoptosis, and 2) when endothelial cells were adhered to a surface through antibodies that bound non-integrin receptors these cells were also susceptible to apoptosis.^[44] Additionally, integrin signalling converges with growth factor signalling during cell proliferation. Specifically, without appropriate integrin signals, cells do not progress from the G1 phase to the S phase of the cell cycle and thus are unable to proliferate.^[45, 46] Furthermore, integrin signalling is also critical in cellular differentiation. For example, the differentiation of myofibroblasts by transforming growth factor- β 1 was found to be dependent on integrin signaling via FAK, and recently Gomez-Lamarca et al. showed that epithelial differentiation is regulated by integrins that modulate Notch activity.^[47, 48]

When cells are cultured on fibronectin, they exhibit a full adhesion response that includes the formation of integrin-mediated adhesion complexes that contain proteins such as talin, α -actin, paxillin, vinculin, F-actin, and filamin.^[33] Additionally, tyrosine phosphorylation events occur within the complexes illustrating signalling events.^[36] A key contribution by Miyamoto is that integrins must be both occupied by ligands and clustered within the cell

membrane in order to exhibit this full adhesion response. To illustrate this, fibroblast-like cells were studied under three different conditions.^[26] The first set of cells was incubated with monovalent and solubilized RGD peptide. These ligands occupied the integrin receptors and resulted in receptor redistribution but minimal tyrosine phosphorylation. The second set of cells was incubated with beads coated with a non-inhibitory monoclonal antibody. These multivalent beads act to cluster the integrins within the cell membrane without affecting the receptors' ability to bind a ligand. However, since no ligand was present, these integrins remained unoccupied. Cells incubated under these conditions showed accumulation of tensin and FAK and signalling through tyrosine phosphorylation. However, only cells that were incubated with the beads and the solubilized RGD peptide mimicked the full adhesion response of cells cultured on fibronectin through the recruitment of all the above-mentioned cytosolic proteins and tyrosine phosphorylation (**Figure 1B**).^[26]

This insightful study shed new light on the biophysics of cell/ECM interactions. However, biomaterial scientists and tissue engineers can learn additional lessons from this work. Until this time, biomaterial surfaces were generally randomly decorated with integrin-binding ligands.^[19] This new knowledge means that a researcher has the possibility of improving the function of cells adhering to a biomaterial by engineering interfaces that both occupy integrin receptors and aid their clustering. However, achieving the required nano-scale patterning of the cell adhesive ligands is not a trivial task and requires the development of new materials fabrication techniques. The development of these techniques is the focus of section 3 below.

3. Fabrication of Biomaterials that Display Multivalent Ligands to Promote Integrin Occupancy and Clustering

The canonical method of biofunctionalizing a cell culture surface is to randomly decorate a non-fouling interface with cell adhesive ligands. In this instance, controlling one parameter, the global density of ligands present at the interface, modulates the bioactivity of the surface (**Figure 1C**). However, this random distribution of ligands only promotes integrin occupancy, not integrin clustering. To generate biomaterials that promote both integrin occupancy and clustering, researchers use multivalent ligands, where the ligands are clustered within a nano-scale “island” (**Figure 1D**). This change in paradigm provides a biomaterials scientist with additional variables that can be used to manipulate cell functions. For instance, instead of simply changing the *global density* of ligand, the ligands can now be partitioned into clusters of various sizes to control the *local density* (**Figure 2**). This additional level of control then prompts questions such as, what is the optimum local ligand density per island? What is the optimum spacing between islands? What is the optimal spacing of ligands within an island? What new cell behaviours can we modulate with this additional level of surface control? To answer these questions, a variety of methods have been developed to control the nano-scale presentation of integrin-binding ligands on biomaterial substrates. In this review, we have differentiated these techniques into three main categories as illustrated in **Figure 3**:

1. Blending techniques based on blending of highly functionalized polymer molecules or nanoparticles with a non-functionalized polymer,
2. Nanolithography techniques that enable nanometer-scale control and resolution of individual integrin binding ligands, and
3. Recombinant protein techniques

The methodologies used to produce biomaterials functionalized with multivalent ligands are described in **Table 1**, the key biological interactions with these materials are

presented in **Table 2**, and the advantages and disadvantages of each fabrication technique are compiled in **Table 3**.

3.1. Blending Strategies

The first generations of materials displaying multivalent ligands were polymeric in nature. Traditionally, a polymer would be synthesized that contains a certain number of reactive sites, and post-synthesis those reactive sites would be functionalized with ligands (**Figure 4A**). Casting the polymer into a thin film or crosslinking the material would result in a cell culture interface that is randomly functionalized with peptide ligand. To achieve the nano-scale clustering of the ligands, the researchers took advantage of the nanometer size of individual polymer molecules. A small portion of polymer would be synthesized with a high degree of ligand incorporation. These highly functionalized polymers would then be blended with non-functionalized materials. Upon film casting or crosslinking, an interface that displays nano-scale clusters of multivalent integrin binding ligands is generated (**Figure 4B**). The average spacing between multivalent islands of ligands can be changed by controlling the blending ratio of functionalized to non-functionalized material. Additionally, controlling the degree of functionalization of the polymer can change the valency of the ligands.

3.1.1. Star Polymers

The first synthetic cell culture surface to use multivalent integrin-binding ligands was generated by Maheshwari et al.^[49] This material was comprised of star-shaped polymers with approximately 35 polyethylene oxide (PEO) arms each (**Figure 4**). The distal end of each PEO arm was functionalized to enable covalent conjugation to the amine terminus of polypeptides. These star molecules are water-soluble, so researchers covalently tethered them

to a crosslinked PEO hydrogel substrate to produce biofunctionalized cell culture surfaces.

The PEO arms and background resulted in a surface resistant to adsorption of proteins, thus

the biological interactions with these materials is due exclusively to the presence and

arrangement of the RGD peptides. Each star has nanometer-scale diameter, and upon

immobilization to the surface this resulted in nanometer scale islands of clustered ligands.

These RGD-functionalized stars were grafted to the surface in defined dilutions with non-

functionalized star molecules. By varying the number of ligands per star and the percentage

of functionalized stars, the researchers generated surfaces with RGD clusters with an average

of 1, 5, or 9 ligands/island; average centre-to-centre distances between clusters of 6-300 nm;

and a global density of 1,000 – 200,000 ligands/ μm^2 .^[49] It is worth noting that these values

are based on the stoichiometry of the reaction conditions during the grafting step and were

not corroborated experimentally.

The behaviour of WT NR6 fibroblasts was studied on these materials.^[49] These cells are

derived from 3T3 murine fibroblasts, which lack endogenous epidermal growth factor

receptors (EGFR). The WT NR6 line was developed through transfection of 3T3 cells in

order to express human EGFR. These cells enabled the researchers to assess how global

ligand density, local ligand density, and the presence or absence of human EGF affected

cellular behaviour. Specifically, four cellular properties were probed in this study: adhesion

capacity, cytoskeletal arrangement, cell migration speed, and cell adhesion strength.^[49]

The presence of the RGD peptide was sufficient to enable cellular adhesion. However, the

researchers observed large variations in the cytoskeletal arrangement. 25% of cells cultured

on materials with a single ligand per island showed development of well-defined actin stress

fibres and vinculin staining was almost completely absent. In comparison, 75% of cell cultured on islands with 9 ligands exhibited well-defined stress fibres and much greater amounts of vinculin staining. These data confirm the hypothesis that advanced materials functionalized with multivalent ligands are able to promote integrin clustering and facilitate the formation of adhesion complexes.^[49]

Migration speed varied drastically with both the global and local ligand peptide density.^[49] Specifically, greater local density resulted in greater migration speeds, for a given global density. For surfaces bearing a single ligand per island, the maximum migration speed in the absence of EGF was approximately 2 $\mu\text{m/hr}$ while surfaces bearing clusters of 9 ligands per island had cells with a maximal average velocity of approximately 16 $\mu\text{m/hr}$. The presence of EGF increased the migration speed of the cells. For instance, the maximum speed of cells on materials with a single ligand per island increased from 2 to 3 $\mu\text{m/hr}$ while the maximum speed of the cells on the surfaces bearing clusters of 9 ligands increased from 16 to 31 $\mu\text{m/hr}$. These results show crosstalk between integrin signalling and growth factor signalling and that coupling growth factor signalling with smart biomaterial design can synergistically regulate cell behavior.^[49]

The strength of cell-substrate adhesion was also assessed.^[49] Briefly, cells cultured on the various surfaces were exposed to a normal detachment force of 800g for 10 minutes. At a constant global density, cell adhesion strength increased with increasing local density. The biomaterials bearing a single ligand per island were only able to retain 14% of the adherent cells after the detachment test. This is in comparison to 35% of the cells which remained adherent to the biomaterials for islands bearing 9 ligands.^[49]

3.1.2. Comb Copolymers

3.1.2.1. Films of Amphiphilic Comb Polymers can Display Multivalent Ligands for Cell Binding

The star polymers presented in the previous section are water soluble molecules that require a chemical reaction to be immobilized to a cell culture surface.^[49] The next step was to create a water-stable thermoplastic that was both non-fouling and presented multivalent integrin-binding ligands. Irvine et al., synthesized a water insoluble, linear, and amphiphilic polymer via free radical polymerization. The comb polymer was polymerized from methyl methacrylate and a methacrylate bearing a PEO pendant group. The hydrophobic methyl methacrylate repeat units enabled water-stable films of polymer to be produced, while the presence of the PEO pendant groups resulted in a non-fouling interface (**Figure 5**).^[50] RGD ligands were coupled to the polymer chains through N-hydroxysuccinimide chemistry.^[50, 51] Variation in the peptide content of the functionalized polymers was obtained by changing the peptide to polymer ratio during coupling. A series of polymers was prepared that contained an average of 1.7 - 5.4 peptides per polymer chain.^[50, 51]

The average global ligand density was tuned by blending functionalized with non-functionalized polymers. Polymer films were produced with bulk peptide density ranging from 12.4 - 50.9 μg peptide/mg polymer. It was assumed that polymers would form a random coil structure and that the functionalized polymer chains would be randomly distributed over the surface of the material (**Figure 5**). As with the stars, the size of the islands would be controlled by the functionalized polymer's molecular size (width of the random coil, ~ 32

nm) and the distance between islands (controlled via blending with non-functionalized polymers) ranged from ~ 50 - 300 nm.^[50]

A significant drawback of all blending techniques is that the characteristics of the biofunctionalized interfaces are difficult to assess directly. The researchers employed both modelling and experimental techniques to confirm the assumption that the PEO pendant groups segregated to the surface and that the peptides were displayed in a nano-scale, multivalent fashion.^[50] First, a self-consistent mean field model predicted a quasi-2D configuration of the comb polymer at the aqueous interface in which the hydrophobic backbone aligned parallel to the interface and the PEO side chains extended into the aqueous cell culture environment. The modelling predicted that the outermost 10 Å of the polymer film was covered by PEO side chains.^[50]

This modeling was supported by two main experimental methods.^[50] First, fluorescent nanoparticles (~ 30 nm in diameter) were covalently coupled with lysine residues present within the peptides exposed at the surface. Upon removal of unattached particles, the fluorescent signal from the surfaces was measured and the number of particles per unit surface area was quantified. The surface density of RGD clusters was determined to be 0- 4.5×10^{10} clusters/cm² with peptide global surface densities of 0-5500 ligand/μm².^[50] In the second study, individual repeat units exposed at the surface to which peptide ligands could be attached were covalently linked to 1.4 nm diameter gold nanoparticles, and the distribution of the particles on the surface was visualized with transmission electron microscopy.^[52] The TEM image showed clustering of the nanoparticles on the surface (**Figure 6**).^[52]

WT NR6 fibroblast cells were cultured on these surfaces and cell attachment^[50] and cell adhesion strength^[51] were assessed. The cells were capable of attaching to the RGD-functionalized interfaces, showing the availability of the peptide ligands for cell binding.^[50] A centrifugal detachment assay was used to measure the adhesion strength of the cells to the substrates.^[51] The number of cells that remained adhered to the surfaces after exposure to a normal detachment force between 0 – 1200 pN/cell was quantified. On surfaces with 1.7 peptides/comb, increasing the detachment force resulted in fewer cells remaining on the surface at the end of the experiment. However, the researchers made a surprising observation; a peak in the adhesion strength profile was detected on the surfaces with 3.6 and 5.4 peptides/comb. This implied that the ligand clustering was resulting in an “adhesion reinforcement” observed within a range of detachment force range between 70 to 150 pN/cell.^[51]

3.1.2.2. *The Architecture of the Comb Polymers Can be Optimized to Facilitate Integrin Clustering*

The comb polymers used above have relatively short PEO pendant groups (6 EO units). The researchers hypothesized that longer PEO tethers would improve the ability of the cells to reorganize the ligands and thus improve their ability to form adhesion complexes. To test this hypothesis, comb polymers with tethers of either 10 EO units (6.5 nm) or 22 EO units (14.3 nm) were synthesized.^[53] These polymers were functionalized with peptides that contain the integrin recognition site (RGD) and a synergy sequence (PHSRN), hereafter referred to as synKRGD (Figure 7). ¹²⁵I-labelled peptides were used to enable quantification of peptide density through radiolabeling measurements, and the peptide surface density was found to vary from 1700 to 2900 peptides/ μm^2 .^[53]

WT NR6 fibroblast adhesion and spreading on the polymer surfaces was explored after 180 minutes of incubation.^[53] The rate of cell attachment and spreading were both greater on surfaces with ligands attached via longer tethers. Additionally, the time required for cells to form focal adhesions decreased. The researchers hypothesized that the greater mobility of the ligands attached to longer tethers enabled the cells to more easily adhere, spread, and form adhesion complexes on these surfaces. To confirm this hypothesis, fluorescence resonance energy transfer (FRET) analysis was used to determine the average separation distance between integrin-bound ligands. For comb polymers with longer tethers, the mean separation distance was 15.6 nm compared to 17.5 nm on polymers with shorter tethers. These results suggest that the added mobility provided by the longer tethers facilitates focal adhesion formation by enabling the reorganization of the peptides.^[53]

3.1.2.3 Comb Polymers can be Blended with Standard Biomaterials and Impart Bio-specific Surface Functionality

Surface modification of many common biodegradable biomaterials, such as polylactide (PLA), is challenging. Additionally, without modification these surfaces exhibit uncontrolled cellular responses arising from protein adsorption. To address these technological shortcomings, researchers blended PLA with comb polymer.^[54] The researchers hypothesized that the comb polymer would partition to the interface, the PEO chains would form a non-fouling coating on the surface, and the ligands would elicit integrin-specific adhesion. This would provide a facile method for controlling/functionalizing the surface properties of this standard biomaterial, both as a film and as 3D tissue scaffolds.^[54]

Both modelling and experiments were used to verify these hypotheses. First, a self-consistent field lattice model predicted the structure of the interface. The model predicted that comb molecules organized in quasi-2D conformations with the strong enrichment of the comb in the top 50 Å of the blends.^[54] Experimentally, blends containing 1 – 20 wt% of the comb copolymer with PLA were produced. Both contact angle measurements and X-ray photoelectron spectroscopy revealed surface segregation of comb polymers when annealed in an aqueous environment. Additionally, polystyrene nanoparticles were covalently attached to the peptides present at the biomaterial's surface and imaged via atomic force microscopy (AFM). The surface density of multivalent ligands was found to vary from 0 to ~1000 clusters/ μm^2 and the total number of RGD ligands at the surface ranged from 0 to about 5500 ligands/ μm^2 .^[54]

WT NR6 fibroblasts were cultured on the surfaces and the adherent cells were imaged with phase contrast microscopy.^[54] The nonfouling properties of the PLA/comb blends were not as good as those of pure comb polymers. However, for blends containing 20 wt % of the comb polymer, only 5% of the seeded cells were able to adhere to the surface. For the largely non-fouling blends, increasing the RGD content resulted in an increase in cell adhesion, and an RGD surface density of ~1500 ligands/ μm^2 was sufficient to enable adhesion similar to that observed on tissue culture plastic.^[54]

3.1.2.4. Nano-scale Clustering of Integrin Binding Ligands Regulates Endothelial Cells Behavior and Are Promising Materials for Blood Contacting Biomaterial Applications

The lack of a blood compatible interface remains one of the most long standing and persistent problems in the biomaterials field. Blood will clot on the surface of most cardiovascular devices and can lead to failure of the device or a portion of the clot can embolize and cause

problems downstream such as stroke. Developing materials that promote the formation of a confluent and functioning endothelial cell layer is an attractive strategy for producing blood-compatible interfaces as these cells are responsible for blood compatibility.^[55] Karimi, et al.^[56] utilized comb copolymers to assess how nano-scale clustering of integrin binding ligands impact endothelial cell behavior. In this work, the authors produced comb copolymers of methyl methacrylate (MMA)/polyethylene glycol methacrylate (PEGMA)/acrylate-PEG-RGD using reversible addition-fragmentation chain transfer (RAFT) polymerization. RAFT polymerization was used to produce polymers of low polydispersity, thus enabling better control over the number of ligands per island. By blending peptide functionalized polymer with non-functionalized polymer, a series of non-fouling materials was prepared with global peptide density ranging from 0.4 to 4.4 μg peptide per mg polymer and local peptide density of 0 to 2.4 peptides per island.^[56]

Human umbilical vein endothelial cells (HUVECs) were cultured on these surfaces and cell adhesion, proliferation, and migration were assessed.^[56] Cell adhesion, endothelialization rate, and migration speed were all maximal on surfaces with the highest global and local peptide density. These results indicate that the ligand clustering can regulate endothelial cell adhesion, migration, and endothelialization rate, and support the idea of using nanoscale ligand presentation to improve the endothelialization of cardiovascular biomaterials.^[56]

3.1.2.5. Conclusions from Star and Comb Polymer Studies

These studies were the first to illustrate that biomaterials can be functionalized with multivalent ligands, and that these surfaces regulate cellular behaviours in ways that cannot be achieved through the canonical method of randomly decorating biomaterial surfaces with single integrin-binding groups. Specifically, the researchers illustrated that attachment,

spreading, cytoskeletal arrangement, focal adhesion formation, adhesion strength, and migration speed of adherent cells can be increased. More intriguingly, the researchers illustrated that the material surface can be tuned to provide a synergistic affect with growth factor signalling. However, in order to obtain these improvements in cellular function, the global ligand density, local ligand density, and availability of the ligand for binding and rearrangement by the cell must be engineered.

The results from these studies can inform the design of future healthcare materials. For instance, the Heath group is already exploring ligand multivalency as a means of improving endothelialization of cardiovascular biomedical implants.^[56] This is a particularly appealing strategy as multivalent ligands improve the adhesion strength of cells to an interface,^[51] and could result in surfaces that more tightly hold endothelial cells when confronted with detachment forces from shear flow. Additionally, cellular infiltration into tissue engineering scaffolds is often desired. By using multivalent ligands, the migration speed of multiple cell types was significantly increased.^[49, 56] Thus, these systems could provide a means of increasing autologous cell recruitment into biomaterials/tissue engineering scaffolds.

3.1.3. Alginate Hydrogels

3.1.3.1. Alginate Hydrogels Functionalized with Nano-clustered Ligands can Improve Cell Proliferation, Differentiation, and Focal Adhesion Kinase Phosphorylation

Mooney and Linderman developed alginate hydrogels that are functionalized with multivalent ligands. Alginate is a linear anionic polysaccharide that forms a hydrogel when ionically crosslinked with divalent cations. These hydrogels have high water content, lack intrinsic cell binding capacity, and resist protein adsorption and cell adhesion unless

modified. These qualities make alginate an excellent background on which to study the effects of multivalent ligands.

Biofunctionalization was achieved by reacting carboxylic acid groups present on the sodium alginate chains to the amine termini of RGD-containing peptides using sulfo-NHS/EDC chemistry. Varying the ratio of peptide to alginate chains during the coupling reaction controlled the number of peptides bound to a single alginate chain, and alginate chains containing an average of 1 – 25 ligands were prepared. The functionalized alginate chains were blended with varying ratios of non-functionalized chains and crosslinked through the addition of calcium sulphate. The size of the peptide-containing islands was controlled by the size of the functionalized alginate chains (~36 nm). The blending strategy allowed the researchers to control the average RGD island spacing from 36 – 168 nm as predicted by a 2D Monte Carlo simulation, and the bulk RGD density in the gels was varied between 0.125 and 80 μg RGD/mg alginate (**Figure 8**).^[57-62]

The impact of ligand multivalency was assessed using three cell types: mouse preosteoblasts (MC3T3-E1 cells), primary human fibroblasts, and myoblasts (C2C12 cells and primary skeletal muscle cells).^[57-60] Proliferation rate, differentiation capacity, and intracellular signalling were explored for the preosteoblasts.^[57, 58] The cell growth rate increased as the bulk peptide density increased; however, the valency of the ligands did not dramatically influence the growth rate at a given global peptide density. Osteogenic differentiation was assessed for cells encapsulated in hydrogel beads. Osteogenesis was significantly increased on hydrogels with more closely spaced islands of ligands compared to gels with larger spacing between islands for a given global peptide density.^[57] Similarly, FAK

phosphorylation increased with increasing bulk density of peptide within the gel, and the phosphorylation was greatest for islands that were more closely spaced.^[58]

Primary human fibroblasts exhibited increased proliferation with increasing global peptide density and reached a plateau at 12.5 μg peptide/mg alginate.^[59] Additionally, the cell growth rate increased with decreasing island spacing for a given peptide concentration.^[59] Myoblast cells (C2C12 cells and primary skeletal muscle cells) were cultured on gels functionalized with either linear or cyclic RGD peptides.^[60] The proliferation of both myoblast cell types increased with increasing global peptide density. The choice of ligand did not affect the initial adhesion of the cells; however, both cell types exhibited higher proliferation on surfaces functionalized with cyclic RGD.^[60]

3.1.3.2 Nano-clustering of Peptide Ligands and Substrate Stiffness can be Independently Tuned to Cooperatively Improve Cell Proliferation

The use of alginate hydrogels enabled facile control of the stiffness of the cell culture substrates. This enabled the researchers to probe the response surface of peptide organization and matrix stiffness on cell behaviour. A range of 2 – 20 RGD peptides per alginate chain was explored, the global peptide density ranged from 1.25 – 12.5 $\mu\text{g}/\text{mg}$ of alginate, and the range of island spacing varied from 36-120 nm. Gels of varying stiffness were prepared, and the resulting hydrogels had compressive moduli of 20-110 kPa.^[61]

The impact of ligand organization and substrate stiffness on MC3T3-E1 murine preosteoblast cells and human bone marrow stromal cells was explored. Cells were able to adhere with the classic spindle shape morphology to the RGD-containing materials. At a given substrate stiffness, both global peptide density and island spacing affected the growth rate of the cells.

Specifically, proliferation increased with increasing bulk peptide density, and the proliferation rate also increased when the island spacing was decreased.^[61] The stiffness of hydrogels played a crucial role in the growth rate of MC3T3-E1 cells. At a constant global and local peptide density the growth rate of preosteoblasts and mesenchymal stem cells was increased with hydrogel stiffness indicating that substrate properties can be tuned with ligand presentation to enhance specific cellular behaviours.^[61]

3.1.3.3. Nano-clustering of Peptide Ligands can Improve Nonviral Gene Delivery and Gene Expression

The nanoscale presentation of peptide ligands was also used to improve nonviral gene delivery and gene expression levels in preosteoblasts.^[62] Alginate hydrogels with bulk peptide densities ranging from 3,000 to 60,000 ligands/ μm^2 were produced. Spreading, actin filament formation, and cell proliferation of preosteoblasts on these surfaces were assessed. The peptide density did not significantly affect the number of adherent cells or the degree of cell spreading over the range of ligand concentrations studied. However, cell proliferation and actin stress fiber formation were increased with increased global RGD density and decreased spacing between islands.^[62]

Condensed nanosize pDNA was prepared by encoding pDNA for luciferase protein and condensing with poly(ethyleneimine).^[62] The pDNA was labelled with rhodamine to quantify the efficiency of gene transfer. Preosteoblasts being cultured on alginate hydrogels with a bulk peptide density of 6,000 RGD/ μm^2 were transfected, and it was shown that the efficiency of gene transfer and the expression levels of luciferase increased as spacing between islands of ligand decreased, in both 2D and 3D hydrogels.^[62]

3.1.3.4. Simulation Provides Deeper Understanding of How Ligand Presentation Affects Cell Behaviour

A freely jointed chain model was developed to predict the ligand distribution within an individual island and the equilibrium chain conformation within the hydrogels.^[63] The model predicts that the RGD ligand spacing within an island increases by increasing the molecular weight of the alginate chain and decreasing the number of ligands per chain, as was to be expected. Additionally, the model predicts that the fraction of ligands that are accessible by cell receptors is only dependent on the chain molecular weight, and this fraction increases non-linearly with increasing penetration depth of the integrin receptors into the alginate surface.^[63]

In a second modeling study, a stochastic Monte Carlo model was developed to predict various responses by MC3T3 preosteoblasts on the functionalized alginate hydrogels.^[64]

Specifically, the interplay between integrin organization, cell spreading, FAK phosphorylation, and osteogenic differentiation was modelled. Forty different ligand nanopatterns were simulated. The surfaces had islands containing between 1 and 15 peptides/chain, and the percentage of polymer chains at the interface that were functionalized with RGD ranged from 10 to 70%. In this model, a 2D “adhesive surface” lattice containing adhesion ligands was overlaid with a second “cell membrane” lattice containing integrin receptors. Three parameters were used to quantify integrin organization: *integrin bound*, meaning the number of integrins bound to a ligand, *contact number* as a measure of short-range organization of the integrin with the clusters, and *bound number density fluctuation* (BNDF) as a measure of the distribution of clusters. The simulation predicted that cell

spreading correlates with the contact number and BNDF; FAK phosphorylation correlates inversely with contact number and BNDF, and increased with formation of the small and homogeneously distributed clusters of integrin; and osteogenic differentiation correlates with high levels of contact number and BNDF, and increases with formation of large and heterogeneously distributed integrin clusters.^[64]

3.1.3.5. Simulation Illustrates that Both Integrin Dimerization and Ligand Organization are Key Components in the Formation of Integrin Clusters.

Brinkerhoff and Linderman gained key insights into the biophysics of integrin cluster formation through the use of Monte Carlo simulation.^[65] Experimentally, it has been found that unbound integrins show a propensity to dimerize due to weak yet rapidly forming interactions, even in the absence of ligand binding.^[65] For example, both β_1 and β_2 subunits have been observed to self-associate on the cell surface.^[66, 67] Interestingly, these weak interactions enable the oligomerization of integrin receptors via the process of partner switching. The formation and disassociation of these integrin-integrin associations is faster than the rate of diffusion of the integrins within the cell membranes. This means that the dimerization of integrins can act to aggregate more than two integrins by switching between integrin partners faster than the individual integrin receptors can diffuse away. From a kinetic point of view, the reaction is diffusion limited.^[65]

Brinkerhoff and Linderman created two parallel 2D lattices separated by 30 nm (the separation distance over which integrin binding can occur).^[65] One lattice represented the cell membrane, in which integrin receptors were embedded. The other lattice represented the substrate on which ligands were distributed, in either a random or nanoclustered manner. In

the absence of ligands on the substrate lattice, the researchers found that integrin dimerization resulted in average integrin cluster sizes of 3.1 integrins/cluster. Additionally, ~15% of the clusters were significantly larger, containing more than eight integrins. In simulations where ligand binding occurs but integrin dimerization is absent the researchers found that clustering of the ligands into islands of high density resulted in integrin clustering. However, when both integrin dimerization and ligand clustering were present, the average size of clusters increased substantially from ~4 integrins/cluster to ~9 integrins/cluster. These results illustrate that surfaces functionalized with nanoclusters of ligands work with the biological propensity of integrin receptors to dimerize to produce larger clusters. The researcher hypothesized that these larger structures act as nucleation sites for the formation of stable focal adhesions.^[65]

3.1.3.6. Conclusions from Alginate Hydrogels

These studies show that multivalency of ligands can promote additional cellular behaviours including cell signalling, proliferation rate, gene expression levels, and differentiation capacity; substrate stiffness can be tuned in conjunction with peptide density to promote cell proliferation; and that the effect of local and global ligand density is distinct for different cell types. This is most clearly seen through the proliferation rate of different cell types cultured on these interfaces: preosteoblast proliferation was largely unaffected by the local ligand density, while decreasing island spacing promoted fibroblast and myoblast proliferation. Also, being a hydrogel that can be crosslinked under cytocompatible conditions, the ability to produce three dimensional and cell-laden structures that regulate cell proliferation and differentiation have strong implications in the development of next generation tissue engineering scaffolds. Rapid development of neo-tissue in such scaffolds, as well as lineage-

specific differentiation of stem cells, is often a primary goal of tissue engineering. These results illustrate that ligand multivalency can play a key role in achieving these goals.

3.1.4. Alginate Hydrogels with Gold Nanoparticles

Wang, et al. also used an alginate-based material to assess how multivalent ligands impact cell behaviours.^[68] In this work, the authors produced thiol-functionalized alginate to which they covalently attached ~30 nm gold nanoparticles through the formation of an Au-S bond. The particles were then reacted with cysteine-terminated REDV peptides to introduce biofunctionality. The thiol group of the cysteine reacted with the gold nanoparticles to produce self-assembled monolayers of peptide on the surface of the particles. The nanometer diameter of the particle was used to create the nano-scale clustering of the peptides.^[68] The REDV peptide was selected as it binds the $\alpha_4\beta_1$ integrin that is only present in a small number of cell types, including endothelial cells.^[69] Materials functionalized with this peptide are often used when generating blood-contacting biomaterials as most other commonly occurring blood cell types do not adhere to this peptide, providing surfaces with specificity towards endothelial cells.^[70, 71] The incorporation of the gold nanoparticles enabled facile imaging of the peptide-modified interfaces through TEM. *In vitro*, the nanoclustered materials resulted in increased adhesion of HUVECs, and these surfaces supported a larger number of HUVECs after 7 days of culture. Additionally, these gels were implanted subcutaneously in mice, and the angiogenesis into these gels was assessed after 14 and 21 days post implantation. The gels functionalized with nanoclustered ligands exhibited at least a 20 % increase in vascularization compared to gels functionalized with monovalent ligand.^[68]

Although blending functionalized nanoparticles with a non-fouling polymer is an attractive strategy for generating surfaces with nanoclustered ligands, the experiments described in this

manuscript had several limitations. First, the alginate used in this work had been chemically modified with thiol groups to enable covalent attachment of the nanoparticles. However, the non-fouling properties of the alginate were adversely affected by this chemical modification. Specifically, gels possessing no ligand saw significant adhesion of both HUVECs and fibroblasts indicating that the gels no longer possessed the desired non-fouling properties. This undesired cellular adhesion limits the conclusions that can be drawn from this work. Additionally, the researchers only assessed a single REDV concentration, so trends on how local and global peptide density affect endothelial behaviour cannot be identified. Despite the shortcomings of this study, improving angiogenesis through the use of multivalent ligands is a significant contribution. One of the critical limitations of the tissue engineering field is insufficient vascularization that limits the size and longevity of neo-tissues. Using multivalent ligands to significantly improve the rate of angiogenesis into a neo-tissue is an exciting result for the field of tissue engineering.

3.1.4. Block Copolymers

*3.1.4.1. Polystyrene-*b*-Polyethylene Oxide Copolymers can form Nano-clusters of Peptide Ligands through Phase Segregation.*

Cooper-White pioneered a method for generating multivalent ligands using commercially available diblock copolymers composed of blocks of hydrophobic polystyrene (PS) and blocks of hydrophilic polyethylene oxide (PEO). When films of these polymers are spin cast, the polymer undergoes phase segregation, and creates a surface with nano-domains of PEO dispersed within the PS continuous phase. Varying the lengths of the PS and PEO segments can be used to vary the number and the size of PEO domains **(Figure 9)**.^[72]

Films of approximately 40 nm thickness were spin cast from three block copolymer solutions: low molecular weight copolymer ($M_n = 62.5$ kDa), medium molecular weight copolymer ($M_n = 136$ kDa), and high molecular weight copolymer ($M_n = 238$ kDa).^[73] AFM analysis confirmed nanoscale phase separation of PEO for all polymers in an aqueous environment, and the size and distribution of the PEO domains varied with polymer molecular weight. By decreasing the molecular weight of the copolymer, the surface coverage of PEO increased from 15% to 59%, the PEO domain size decreased from 51 to 29 nm, and the surface density of PEO domains increased from 73 to 907 domains/ μm^2 .^[73] According to the AFM analysis, a maximum of 59% of the surface was covered with PEO.^[73] Surprisingly, this incomplete coverage was sufficient to reduce protein adsorption and eliminate cell adhesion. The low molecular weight copolymers, with approximately 900 islands/ μm^2 , were used as a low-fouling background for the immobilization of bioactive ligands.^[73]

Peptide ligands were incorporated onto PEO blocks by functionalizing the terminal hydroxyl group with either an RGD-containing peptide or a fibronectin type III fragment that spans the 7th to 10th repeat units (FNIII₇₋₁₀).^[74] A large number of NIH-3T3 fibroblast cells adhered to the surfaces functionalized with the RGD peptide compared to the fibronectin fragment.^[74] The diameter of the nano-domains was approximately 30 – 50 nm, while the diameter of a single integrin receptor is approximately 10 nm. This means that it is theoretically possible for multiple integrins to access ligands present on a single domain, and one could envision that this would facilitate the formation of adhesion complexes. However, the clustering of integrins was not investigated, nor was any improvement in cellular phenotype reported on these surfaces. Additionally, no analysis was presented to estimate the number of RGD sites

per nano-domain, meaning that both the bulk and local density of RGD on the surface is uncertain.

A second generation of surfaces baring nano-clustered ligands was developed using the same block copolymers by covalently modifying the terminal hydroxyl group of the PEO blocks with an adamantane moiety.^[75] Adamantane groups can act as the “guest” in inclusion complexes with β -cyclodextrin. These adamantane-functionalized polymers now exhibited facile conjugation with cyclodextrin-modified molecules. The adamantane-functionalized polymers were then blended with non-functionalized block copolymers to control the amount of peptide that could couple to the surface of the biomaterial. The researchers attached cyclodextrin-modified peptides to the adamantane-functionalized surfaces. Specifically, two peptide sequences were explored, an RGD-containing peptide and an IKVAV-containing peptide derived from laminin.^[75]

The initial (2 hour) adhesion and morphology of human mesenchymal stem cells (MSC) were explored.^[75] The initial adhesion of MSC was found to increase with increasing RGD content at the interface until the blend ratio reached 50% after which no further increase in cell adhesion occurred. However, cell spread area after increased in a near linear manner with increasing RGD content over all concentrations from approximately 1,000 ligand/ μm^2 to 3,500 ligand/ μm^2 .^[75]

Films of 100% adamantane-functionalized polymer were then grafted with varying molar ratios of the RGD- and IKVAV-peptides (from 0 – 100% RGD).^[75] Regardless of the ratio of the peptides in the material, the number of cells adherent to the surfaces after 2 hours was constant. However, the morphology of the cells was highly different. Specifically, cells on

the surface that contained only IKVAV had a smaller projected cell area (approximately $1,500 \mu\text{m}^2$) that increased nearly linearly with increasing the amount of RGD peptide to approximately $3,500 \mu\text{m}^2$ on surfaces containing only the RGD peptide.^[75]

3.1.4.2. The Lateral Spacing of Peptide Ligands can Modulate Adhesion and Differentiation of Mesenchymal Stem Cells

In order to generate surfaces that presented different densities of PEO domains (and thus different densities of RGD after functionalization) films were created by blending 0-100 % of a functionalized copolymer with a polystyrene homopolymer.^[76] The average size of the PEO nano-domains was 8 - 14 nm for all blends, and the average space between domains ranged from 34 – 62 nm. Through radius of gyration calculations, it was estimated that six PEO tethers were clustered together in each of the PEO domains. Films were then functionalized with an RGD-containing peptide.^[76]

This blending strategy introduces two major limitations into the system. Blending the copolymers with polystyrene incorporates greater amounts of hydrophobic material into the films that can adsorb protein from the solution phase. Subsequent cell adhesion experiments were conducted over short times in serum free media. For long term studies or studies with serum, the surface would need to be blocked through the adsorption of a non-fouling molecule such as albumin or a Pluronic. Additionally, the blending reduced the size of the PEO domains to a maximum of 14 nm. An integrin receptor has a diameter of approximately 10 nm. It is unlikely that multiple integrins would be able to attach to a single PEO domain. Therefore, studies using this surface no longer promote clustering of the integrins, but instead enabled the researchers to assess the effects of lateral spacing between ligands.

To assess the effect of the lateral spacing of RGD on the behaviour of MSC, the cells were seeded onto these surfaces for up to 24 hours in serum-free media.^[76] MSC morphology was strongly affected by the spacing of the RGD. For closely spaced clusters of ligands, cell area, formation of stress fibers, and the formation of mature focal adhesion complexes (length of 10 μm or longer) were increased.^[76] The migration, osteogenic, and adipogenic differentiation of the cells were also assessed.^[76] Cell migration speed exhibited a biphasic response as the lateral spacing between ligands was varied. Specifically, the migration rate of the MSC exhibited a maximum when the spacing between RGD domains was 50 nm. The researchers rationalized this as a substrate with intermediate adhesion strength allowed firm cell adhesion, but was not so adhesive that it prevented cellular motion. In order to investigate the osteogenic and adipogenic differentiation of MSC, the cells were cultured on the surfaces for 4 hours in serum-free media and then incubated in osteogenic and adipogenic media. Differentiation was probed through quantitative real-time PCR (qPCR) and expression of lineage specific markers (alkaline phosphatase and lipoprotein lipase, respectively). As the distance between PEO domains increased, osteogenic differentiation was found to decrease and adipogenic differentiation was found to increase. In order to use these surfaces for long-term cell culture studies, the surfaces were blocked with Synperonic F108 before inoculation with cells.^[76] However, no data was presented to illustrate that the blocking layer remained effective through the duration of the culture.

3.1.4.3. The Regularity of the Interface can be Improved through Incorporation of Perfluoromoietyes.

One limitation of all of these blending strategies is that it is difficult to control the spacing and size of the peptide islands. However, this issue was addressed through the incorporation of hydrophobic perfluoro groups that promoted a more consistent phase segregation of the

polymer, resulting in an interface with very regular size and spacing of the PEO domains.

This was accomplished by synthesizing a block terpolymer through anionic polymerization containing a block of polystyrene and a block of copolymerized polyethylene oxide and allyl glycidyl ether (AGE, 3% of AGE relative to EO). The AGE groups enable facile functionalization through a thiol reaction. These polymers were then functionalized with a 1:1 mixture of an RGD peptide and the hydrophobic perfluorooctanethiol. After spin casting and annealing, these materials exhibited a very regular hexagonal packing of the bio-functionalized PEO domains as observed through AFM imaging. These results illustrate that stable and well-defined nanostructured substrates can be generated by modification of block copolymer via a perfluoro-moiety.^[77] Cell culture with 3T3 fibroblasts showed strong vinculin staining, well-formed actin filaments, and more discrete focal adhesions on these surfaces, demonstrating the strong adhesion of the cells on these surfaces.^[77]

3.1.4.4. Conclusions from Block Copolymer Studies

The major advantage of the block copolymer system is the ability to directly assess the size and distribution of the PEO domains, and thus better determine the distribution of RGD ligands across the surface. Additionally, the adamantane-functionalization chemistry provides a facile method for incorporating a wide variety of functional groups onto a single biomaterial platform. The most significant cellular insight gained from this work is that the lateral spacing of ligands can be tailored to promote lineage-specific differentiation of mesenchymal stem cells, a finding that adds additional evidence to the claim that ligand nano-spacing can be used in the design of future tissue engineering scaffolds.

Despite the ability to better characterize these interfaces, the authors feel that this material system is less flexible than the comb polymers or alginate hydrogels. The need to work in

serum free media or to block the surface with a surfactant drastically limits their utility, the need to spin coat these surfaces limits their scalability, and it is likely that this approach is limited to 2D culture systems making it less suitable for the development of 3D tissue scaffolds or complex biomedical devices.

3.2. Nanopatterning

The greatest disadvantage of the blending techniques described above is the ambiguity of the surface and lack of precise spatial control of the cell adhesive ligands. The blending strategies do not enable precise control of the number of ligands per island, the spacing of ligands within the island, or the spacing between islands. These surfaces can illustrate that nanoscale clustering of ligands can be used to promote a variety of desirable cell behaviours; however, they are insufficient to address fundamental biophysical questions such as what is the ideal spacing of ligands within an island, what is the ideal spacing between islands, etc. In order to generate cell culture surfaces with a higher degree of spatial control, two nanolithography techniques have been developed: block copolymer micelle nanolithography and nanoimprint lithography.

3.2.1. Nanoparticle Arrays via Micelle Nanolithography

3.2.1.1. Block Copolymer Micelle Nanolithography Can Generate Surfaces with Nanometer Scale Quasi-hexagonally Packed Peptide Ligands with Well-Controlled Peptide Separation Distances

Spatz and coworkers took advantage of the nanometer scale of the micelle in order to produce planar surfaces patterned with biofunctionalized arrays of gold nanoparticles.^[78] The researchers synthesized a poly(styrene)-*block*-poly(2-vinylpyridine) copolymer through living anionic polymerization and produced micelles with polar cores by dissolving the

polymer in toluene. Using a reduction reaction of tetrachloroaurate (HAuCl_4) with hydrazine, the polar cores of the micelles act as nano-scale compartments in which a single gold nanoparticle forms. When a flat substrate (glass, mica, or silicon) is dipped into and then retracted from a dilute solution of the micelles, a monolayer of micelles forms on the surface and pack into a 2D quasi-hexagonal pattern.^[78]

The polymeric components of the micelles are then removed through exposure to plasma, leaving behind the gold nanoparticles attached to the surface in the same hexagonal pattern (**Figure 10**).^[78] The size of the particles could be varied between 1 and 15 nm depending on the conditions of the reduction reaction, and the interparticle distance could be tuned from 30 to 250 nm by varying the lengths of the copolymer chains, the concentration of micelles in solution, and the retraction rate of the substrate from the micelle solution. This treatment results in a surface covered by an extended pattern of quasi-hexagonally packed gold nanoparticles with defined interparticle spacing. The hexagonally packed arrays of nanoparticles are easily detectable via a variety of imaging techniques including TEM, SEM, and AFM (**Figure 11**).^[78]

Before these substrates could be used for cell culture applications, the gold nanoparticles needed to be functionalized with cell adhesive ligands and the space between particles needed to be passivated with a non-fouling layer to prevent non-specific cellular interactions. In order to passivate the surfaces, the substrates were submerged in a solution of PEG or polyethylene glycol silane.^[79] After thorough rinsing, the gold nanoparticles were reacted with an aqueous solution of a thiol-terminated peptide that contained a bioactive cyclic RGD sequence. The terminal sulfhydryl group of the peptides allowed facile functionalization of the gold nanoparticles through the formation of self assembled monolayers via thiol-gold

chemistry. The diameter of the head of an integrin receptor is 8 – 12 nm. The researcher chose to work with nanoparticles with a diameter < 10 nm so that only a single integrin would be able to bind to single functionalized nanoparticle.^[79] It is important to point out that most of the below studies were performed on extended arrays of nanoparticles meaning that the researchers were assessing the impact of lateral ligand spacing on cell behaviours. It is not until section 3.2.1.9 that the researchers decouple local and global ligand density on these interfaces.

3.2.1.2. Identifying a Critical Spacing between Ligands that Improves Cell Spreading, Focal Adhesion Assembly, Migration Speed, Adhesion Strength, and Lipid Raft Clustering.

Researchers produced RGD-functionalized cell culture surfaces with interparticle distances of 58 nm and 110 nm. Rat embryonic fibroblasts (REF52 fibroblasts) were cultured on the surfaces and their adhesion, spreading, focal adhesion assembly, and adhesion strength were investigated.^[80, 81] Larger numbers of cells were able to adhere on the more densely packed nanoparticle arrays (58 nm), and these cells exhibited a more well spread morphology. The REF52 fibroblast cells were transfected to express green fluorescent protein (GFP)-tagged β_3 integrins. Fluorescence microscopy was used to visualize the distribution of the β_3 integrins within the cell, localization of the focal adhesion molecules vinculin and zyxin, and the development of stress fibers. Only cells cultured on the more densely packed nanoparticle arrays (58 nm) exhibited clustering of the β_3 integrins, colocalization of vinculin and zyxin, and well formed stress fibers indicating that lateral spacing of integrin adhesive ligands affects the ability of cells to form focal adhesions. Additionally, cells spread faster on the more densely packed nanoparticle arrays.^[80, 81] MC3T3 osteoblasts, B16 melanocytes, and 3T3 fibroblasts cultured on surfaces with average lateral distances between ligands of 28, 58, 73, and 85 nm showed similar results.^[79] A lateral spacing of < 73 nm between ligands was

required to improve cell adhesion, increased spreading, and enable formation of focal adhesions and actin stress fibers.^[79-81]

The sensitivity of hematopoietic stem cells (HSCs) to spacing of RGD-ligands was also explored.^[82] Surfaces with lateral spacing of 20, 32, 58, and 90 nm between peptides were prepared. The researchers used fluorescence microscopy to assess the redistribution of lipid rafts, CD34, CD133, integrin $\alpha_v\beta_3$, and α_5 integrins. On the surfaces with ligand spacing of 20 and 32 nm, the cells adhered well, while cell adhesion was highly decreased on the surfaces with 58 and 90 nm. An extensive redistribution of CD133, CD34, lipid raft, $\alpha_v\beta_3$ integrins, and α_5 integrins was induced by cell adhesion to the substrate with 20 and 32 nm spacing between ligands. Additionally, the cells cultured on the more densely packed surfaces exhibited intensified cell signaling. The results showed that the ligand spacing is a critical for cell adhesion, integrin-mediated lipid raft clustering, and signal transduction, and verifies the sensitivity of hematopoietic stem cells to ligand lateral spacing.^[82] However, it is interesting to notice that the critical ligand spacing for the HSCs is less than for the other types of cells explored, indicating that the nanoscale presentation of ligands must be tailored towards a given cell population.

Two AFM studies were performed to measure the adhesion force of cells to the nanoparticle arrays.^[83, 84] In the first study, single REF52 fibroblasts were attached to the tip of AFM cantilevers, the cells were brought into contact with the nanopatterned surfaces, and the detachment force was measured. Four surfaces were explored with interparticle spacing of 35, 55, 70, and 103 nm. The magnitude of the detachment force on the more densely packed arrays (35 and 55 nm) was significantly greater than on the arrays with larger interparticle spacing. For instance, the detachment force of the cells on the 35 nm-spaced arrays was ~2.3

nN compared to ~ 0.3 nN on the 103 nm-spaced array. Additionally, since the detachment force did not vary linearly with the surface density of the binding sites, the authors propose that clustering of the integrins within the membrane observed on the more densely packed nanoarrays acts to reinforce the adhesion of the cells.^[83] In a second AFM study, surfaces with interparticle spacing of 28, 50, 90, and 103 nm were developed.^[84] A fibronectin-coated AFM tip was brought into contact with individual cells on the surface, the AFM tip was allowed to adhere for up to 15 minutes, and then the AFM tip was used to pull the cell from the substrate. A non-linear increase in the detachment force was observed when the ligand spacing was ≤ 50 nm due to the presence of the focal adhesions.^[84]

3.2.1.3. Different Integrin Receptors Play Different Roles in Cell Spreading and Focal Adhesion Formation

Multiple integrins are involved in the cell adhesion and focal adhesion formation including the $\alpha_5\beta_1$ and $\alpha_v\beta_3$ integrins. The nanoparticle arrays were used to decouple the relative contribution of these integrins in initial cell adhesion and spreading events and in focal adhesion formation. In order to accomplish this, planar arrays of nanoparticles were fabricated with 30, 60, or 90 nm separation distances. The nanoparticle arrays were then functionalized with a peptomimetic ligand that only binds the $\alpha_5\beta_1$ integrin or a ligand that only binds the $\alpha_v\beta_3$ integrin.^[81, 85]

When osteosarcoma (U2OS cells) were cultured on these surfaces, the cells were able to adhere and spread, with the greatest amount of spreading occurring on surfaces with the smallest spacing between ligands.^[86] However, the degree of spreading varied greatly between the two ligands. On densely packed surfaces, cells cultured on surfaces functionalized with the $\alpha_5\beta_1$ ligand achieved a projected cell area of $\sim 3000 \mu\text{m}^2$ while cells on

the surfaces functionalized with the $\alpha_v\beta_3$ ligand only achieved a projected area of $\sim 2000 \mu\text{m}^2$. Despite the ability of cells to spread more on the surfaces functionalized with the $\alpha_5\beta_1$ ligand, the cells on surfaces functionalized with the $\alpha_v\beta_3$ ligand formed larger focal adhesions. Additionally, when the $\alpha_v\beta_3$ integrin is blocked through addition of the soluble ligand, the cells exhibit decreased focal adhesion assembly. These results indicate that binding of either the $\alpha_5\beta_1$ or the $\alpha_v\beta_3$ is sufficient for cell adhesion; however, the activation of the $\alpha_v\beta_3$ integrin is critical for formation of stable focal adhesions.^[86]

3.2.1.4. Cell-cell Interactions are Affected by Substrate Ligand Presentation

Researchers use micelle nanolithography to prepared surfaces patterned with 10 nm particles with a particle spacing of 57 nm.^[87] The surfaces were passivated and functionalized with an RGD-containing ligand as described previously, with one exception. The nanoparticles were also conjugated with a photocleavable PEO-thiol. Before exposure to UV radiation, the photocleavable PEO group hid the RGD-peptide from view of cells resulting in non-fouling interface. However, when regions of the surface were irradiated the PEO groups were cleaved, cells were able access the RGD-peptides, and cell adhesion occurred in a spatially controlled manner. After cells were adhered to the surfaces, additional UV irradiation steps could be performed to make new areas of the cell culture surface available for cell adhesion. These photoactivated surfaces were used to assess how ligand spacing affected migration of HeLa cells. The migration behaviour of the cells on the nanopatterned surfaces was compared to planar surfaces of gold that had been homogeneously functionalized with the RGD-peptide and the photocleavable PEO.^[87]

First, circular cell-adhesive regions were created through UV exposure.^[87] After cell seeding, approximately 20 – 25 cells were capable of adhering per region, and cells were allowed to

incubate for 9 hours in order to generate both cell-substrate and cell-cell interactions. A second irradiation step was used to expose the RGD-peptides in the area immediately around the cells, and cells were then able to migrate into the newly exposed region. Cell migration behavior varied based on the substrate. On homogenous surface, the cells migrated more collectively from the center outwards while keeping their cell-cell contacts. However, on the nanopatterned surface, many cells lost their cell-cell contacts and started to migrate more as individuals. Additionally, the cells migrated at a higher rate and lower average directional persistence on these nanopatterned surfaces.^[87]

3.2.1.5. Melanoma Cell Behavior Determine by Nanoscale Integrin Ligand Patterns

The behavior of four human melanoma cell lines (A375, MeWo, LOX, and MelHO) was investigated on nanopatterned surfaces with ligand spacing of 30 to 120 nm.^[88] As with other cell types, ligand spacing regulated cell adhesion, spreading, focal adhesion assembly, and actin stress fiber formation. Additionally, the optimum ligand surface density was observed to be ~ 350 ligands/ μm^2 . At higher ligand spacing, the cells showed reduced adhesion capacity, and at significantly higher ligand density (~ 1150 ligands/ μm^2) exhibited difficulty in spreading and focal adhesion formation, potentially due to steric hindrance.^[88]

Beyond the identification of the biophysical constraints for focal adhesion formation, the nanopatterned interfaces also enabled insight into the seemingly paradoxical effects that antitumor therapies can have on tumor progression. Specifically, the spreading of melanoma is aided by an overexpression of certain integrins including $\alpha_v\beta_3$. As such, antitumor drugs such as cilengitide that target integrin receptors have been trialed. Preclinical trials of the drug demonstrated good efficacy against melanoma cells; however, a recent phase II clinical trial showed that low doses of cilengitide could paradoxically enhance tumor growth. The

researchers exposed the melanoma cells to soluble RGD peptides prior to seeding onto the nanopatterned surfaces to mimic the impact of the antitumor drug.^[88] The low dose of RGD was found to make the more densely packed surfaces more hospitable to the adhesion and spreading of the tumor cells as observed by increased spreading and focal adhesion formation, likely by limiting the number of integrin receptors that were available for binding to the micropatterned surface. The authors hypothesize that this is mimetic of the *in vivo* mechanism that leads to paradoxical tumor growth when treated with low dose anti-integrin drugs.^[88]

3.2.1.6. Disorder in the Arrangement of Ligands can Improve Cell Adhesion and Spreading

An advantage of the micelle nanolithography process is the well-defined surface that it produced. However, the experimenters wanted to assess the impact of disorder in the distribution of the ligands on cell behaviour. This was accomplished by dissolving polystyrene homopolymer with the micelles before dip-coating the substrate.^[89] By varying the ratio of the polystyrene to the block copolymer, the spatial arrangement of the micelles on the dip-coated surface was disrupted resulting in disordered arrays of nanoparticles. Eight surfaces were prepared in this study. The first four surfaces were well ordered with inter-particle distances of 55, 70, 94, and 100 nm. The latter four surfaces had disordered arrays of nanodots, but very similar average inter-particle distances, 58, 73, 92, and 101 nm.^[89]

MC3T3-E1 osteoblast cells were seeded on these surfaces and the researchers assessed the number of adherent cells, projected area, morphology, and focal adhesion formation.^[89] The osteoblasts were able to adhere and spread equally well on both the regular and disordered surfaces for the most densely packed particles (inter-ligand spacing of 55 or 58 nm).

However, at larger inter-particle distances, the disordered surfaces were able to adhere larger

number of cells and those cells were more spread and possessed thicker actin filaments and stronger vinculin staining. The authors rationalize these interesting results by stating that although the average ligand density is over the critical ligand spacing for this cell type, the disorder results in some ligands that are within the critical distance between one another. These ligands that happen to be close enough together are sufficient to promote integrin clustering and focal adhesion formation.^[89] These results illustrate that disorder in the spacing of nanoscale islands can be beneficial to cellular adhesion. Additionally, this implies that the inherent non-uniform distribution of multivalent ligands present on the blended surfaces described in section 3.1 may actually be beneficial across certain concentrations of ligand surface density.

3.2.1.7. Cells can Sense Gradients in Ligand Spacing and Migrate in Response

The researchers were able to create surfaces with defined gradients in ligand spacing by varying the retraction rate of the substrate from the micelle solution, the polymer concentration in the micelle solution, and the polymer chain length.^[90, 91] Controlling these three parameters enabled researchers to create substrates where the interparticle spacing varied linearly between 50 and 250 nm. These substrates were functionalized with cyclic RGD. MC3T3 osteoblast cells were cultured on these surfaces and the spreading, focal adhesion formation, actin filament formation, polarization, and migration were explored on the region of the surface where the particle spacing varied from 50 – 80 nm.^[90, 91]

On surfaces without gradients the cells usually spread in a uniform manner with well-developed vinculin staining around the perimeter of the cells and well-established actin stress fibers.^[90, 91] Cells cultured on the gradient substrates, on the other hand, were highly aligned in the direction of the gradient, had thinner stress fibers, and less organized vinculin.

Additionally, the migration behaviour of the cells on the uniform and gradient surfaces was different. The researchers observed that fibroblasts on homogeneous surfaces migrated in a random manner. However, on the gradients, the cells migrated in the direction of smaller interparticle spacing, again demonstrating that the cells can sense and respond to small changes in ligand density.^[90, 91] The change in inter-ligand spacing over the length of a cell is approximately 1 nm. However, this small gradient in ligand surface density was sufficient to elicit cell polarization and directional migration, illustrating that the cells can sense and respond to exquisitely small changes in their environment.

3.2.1.8. Transferring Nanopatterned Arrays to Soft Substrates

A limitation of block copolymer micelle nanolithography is that it is restricted to stiff substrates. To address this issue, the researchers developed a transfer lithography technique that enables the relocation of nanopatterned arrays onto polymeric substrates of varying stiffnesses (**Figure 12**).^[92] Gold nanoparticle arrays are first fabricated on glass or silicon. Then linker molecules (e.g. propene thiol or cysteamine) are covalently linked to the nanopatterned gold particles via thiol chemistry. Next, the linker-functionalized substrates are coated with a polymer melt, polymer solution, or polymer precursor solution. The liquid phase is then solidified through cooling of the melt, evaporation of the solvent, or crosslinking of the precursor solutions, respectively. This step physically or chemically attaches the linker to the polymer. When the polymer layer is removed from the substrate, the gold nanoparticles are also removed, resulting in a polymeric surface covered with a uniform and well-ordered array of nanoparticles. Additionally, the researchers are able to develop nanoparticle arrays on simple non-planar geometries such as glass rods. Upon transfer of the particles to a soft substrate, this resulted in a lumen-like structure decorated with a well-

ordered array of gold nanoparticles that could be functionalized with bioactive peptide ligands.^[92]

For cell studies, nanoparticle arrays were immobilized onto the planar surface of a crosslinked PEO gel (molecular weight between crosslinks of 700 Da) that was a largely non-fouling surface.^[92] After functionalizing the nanoparticles with an RGD-containing peptide, the adhesion and spreading of 3T3 fibroblasts on surfaces with ligand spacing of 40, 80, and 100 nm were explored. Robust cell adhesion was seen on the surfaces with 40 nm spacing between particles, but was significantly diminished on substrates with larger spacing between particles illustrating that the gold nanoparticles can be functionalized after the transfer step and that these ligands are available for cell binding.^[92]

In a separate study, murine MSCs were plated on a planar PEO hydrogels with interparticle spacing of 37, 53, 77, 87, and 124 nm between RGD ligands.^[93] Cell adhesion, morphology, and differentiation were investigated. As observed for other cells types, the number of adhered cells and their spreading decreased with increasing ligand spacing. Osteogenic and adipogenic differentiation of cells was assessed after seven days of induction. Interestingly, larger spaces between ligands increased the efficiency of both osteogenic and adipogenic differentiation over the range of particle spacing studied.^[93] The osteogenic results are contrary to what was reported by Cooper-White who illustrated a decrease in osteogenesis with increasing lateral spacing between ligands.^[76] Unfortunately, more experiments were not performed to assess the interplay between ligand distribution and substrate modulus.

3.2.1.9. Decoupling the Impact of Global and Local Ligand Density on Nanopatterned Surfaces using Electron Beam Lithography

The micelle nanolithography process produces surfaces that are covered with extended patterns of evenly spaced ligands. Thus, as the local density is increased (by decreasing the spacing between nanoparticles), the global ligand density also increases. In order to decouple the effects of local and global ligand density, an electron beam lithography approach was utilized.^[94] Briefly, after depositing the micelles on a surface, the desired patterns were traced with e-beam lithography to locally modify the polymer micelles. The polymer and nanoparticles in the non-modified regions could then be removed through sonication in an organic solvent. The remaining micelles were removed through exposure to plasma to leave behind the desired patterns of the nanoparticles (**Figure 13**). Well defined micron-scale regions that are covered with nanoparticle arrays can be generated through this technique.^[94] For cell culture experiments, the researchers generated square patches of 58 nm-spaced nanoparticles that contained between 6 and 3000 particles per patch.^[95]

In their previous studies, the Spatz group showed that many cell types were unable to spread or form focal adhesions on surfaces of extended nanoparticle arrays with a global ligand density of 100 ligands/ μm^2 when the separation between ligands was 85 nm or greater. However, in this work REF52-YFP easily spread, formed focal adhesions, and exhibited well-formed actin stress fibers on these micro-nanostructured interfaces, even though the global ligand density was only 90 ligands/ μm^2 . These results indicate that local ligand density is the key driver of focal adhesion formation and cytoskeletal assembly for these cell types, and that as few as six ligands per island are sufficient to elicit these behaviours.^[95]

3.2.1.10. Conclusions from Micelle Nanolithography Studies

The exquisite nanometer scale control of ligand spacing enabled by the micelle nanolithography technology enabled researchers to gain insight into the fundamental biophysics of cell adhesion, spreading, and focal adhesion formation. For instance, a spacing of 60 nm between adjacent ligands is the maximum to enable focal adhesion formation for many cell types. However, for hematopoietic stem cells, the critical ligand spacing was found to be smaller, 32 nm. Additionally, it was observed that binding of the $\alpha_v\beta_3$ integrin is critical for formation of stable focal adhesions, and that cells can sense and respond to gradients in ligand spacing. These interfaces also shed light on the counterintuitive impact that certain anticancer drugs can have on the progression of cancer *in vivo*.

These results further illustrate the importance of multivalent ligands and their influence on a wide range of cellular behaviours. Additionally, they provide further insight into design of future healthcare materials. The migratory nature of cancer cells on these surfaces is particularly intriguing. Until now, the authors have mostly looked at the future impact of these studies from a tissue engineering point of view. However, these results illustrate that multivalent ligands can also play a key role in the design of future diagnostic and drug testing devices, especially those related to cell adhesion and migration.

3.2.2. Nanoparticle Arrays via Nanoimprint Lithography

Sheetz and Wind developed a nanoimprint lithography (NIL) technique to create nanostructured surfaces to precisely explore the critical density, spacing, and cluster size of integrin adhesive ligand that are essential for eliciting specific cellular behaviors.^[96, 97] This technique enabled the researchers to precisely regulate the local and global density of ligands through the control of factors including the number of ligand per island, the space between

islands, the space between ligands within an island, and the density of ligands. The nanoscale bioarrays were generated through multiple steps (**Figure14**). First, the NIL masks were created by chemical vapor deposition of either hydrogen silsesquioxane or diamond-like carbon on a silicon wafer and patterned by electron beam lithography. The pattern was then imprinted onto a 60 nm thick poly(methyl methacrylate) film that had been spin coated onto a glass or silicon substrate. Once the pattern was transferred, a hard mask of titanium was selectively deposited on the raised features of the PMMA by angled electron beam evaporation, the wafer was then descummed to expose the underlying glass or silicon substrate, gold-palladium (AuPd, 60%/40%, 3 nm thickness) was deposited by electron beam evaporation, lift-off was performed, and thermal annealing was implemented by immersing of the substrate in boiling acetone. The processing resulted in a surface of uniformly spaced spherical AuPd nanoparticles with size of ≤ 10 nm on a background of either glass or silicon.^[96, 97]

Before these materials could be used for cell culture, the nanoparticles needed to be biofunctionalized with cell adhesive ligands and the glass/silicon background needed to be passivated with a non-fouling layer. To accomplish these tasks, the substrates were submerging in a mixed solution of biotinylated ethylene-glycol-undecylthiol and ethylene-glycol-undecylthiol.^[96, 97] The thiol groups formed a self assembled monolayer on the nanoparticles via thiol chemistry. The space between nanodots was passivated via a monolayer of PEG-silane to prevent nonspecific protein adsorption and cell adhesion. The biotinylated nanoparticles were then able to bind a wide variety of molecules via biotin/streptavidin interactions, an interaction that the researchers utilized in order to functionalize the dots with a cyclic RGD peptide. It is likely that more than one ligand was immobilized to each nanoparticle. However, the particles were < 10 nm while the diameter of

an integrin head is 8-12 nm; therefore, it is believed that only one integrin would be able to interact with a single nanoparticle.^[96, 97] By controlling the pattern of the initial NIL mask, the distribution of the resulting nanoparticle array could be finely controlled providing the researchers with exquisite control over the spacing of individual cell adhesive ligands and allow unprecedented control over factors including local and global ligand density, spacing between ligand islands, spacing between individual ligands, etc.

The researchers generated hexagonally packed arrays of nanodots.^[97] The distance between dots in these arrays was varied between 50 and 100 nm. NIH 3T3 fibroblast cells were used to investigate the dynamics of spreading over 3 hours. Essentially all cells were able to spread on the control surface, while cells were only capable of spreading on some of the nanoparticle arrays. Specifically, a large percentage of cells (> 80%) were able to spread on arrays where the distance between dots was less than or equal to 60 nm, or else low levels of spreading (20 – 30%) was observed. The researchers also generated surfaces with islands of nanoparticles to determine the minimum number of ligands that is necessary to support cell spreading. The number of particles per island was varied from 2 to 7 while the global ligand density was held constant at 50 ligands/ μm^2 (the space between each ligand in a given island was 60 nm). A noticeable increase in the percentage of cell spreading was detected between surfaces presenting 3 and 4 ligands per island. Only 50% of the cells on the surfaces with islands of 3 ligands were able to spread, but this value increased to 80% on surfaces with islands of 4 ligands indicating a threshold of local density that must be reached.^[97]

3.3. Bio-inspired Approaches

3.3.1. Protein Chimeras

3.3.1.1. Transfected Bacteria can Be Used to Produce Protein Chimeras

The early work done to produce biomaterials displaying multivalent ligands used synthetic chemistry and lithographic techniques. Kreiner et al. was the first to employ a biotechnology approach in order to produce surfaces functionalized with well-controlled multivalent ligands.^[98] In this work, researchers aimed to make a multivalent ligand that binds the $\alpha_5\beta_1$ integrin.^[99] To accomplish this, protein chimeras containing the 9th and 10th domain of type III fibronectin were produced using transfected *Escherichia coli* (*E. coli*). The protein chimeras contained five key features as shown in **Figure 15**: (1) a polyhistidine tag to enable purification via affinity chromatography; (2) the 9th and 10th domain of fibronectin type III that contain the binding and synergy site; (3) a spacer group based on an IgG hinge to prevent steric hindrance between integrin receptors; (4) a domain based on the GCN4 leucine zipper that enables self assembly of the individual protein chimeras into dimers, trimers, or tetramers via coiled coil interactions; and (5) a C-terminal cysteine. The terminal cysteine was further functionalized with a biotin linker to enable directional attachment of the protein chimeras to avidin-coated substrates.^[98]

The self assembly of these protein chimeras into dimers, trimers and tetramers, and the subsequent purification based on size exclusion chromatography enabled the production of multivalent ligands with a high degree of control over the number of ligands per molecule.^[98] Upon immobilization to a surface pre-adsorbed with avidin, surfaces displaying 2, 3, or 4 binding domains per island were generated. Additionally, baby hamster kidney fibroblasts were incubated on the surfaces. The number of cells with spread morphology was significantly higher for surfaces with larger numbers of ligands per island.^[98] Unfortunately, only initial adhesion and spreading experiments were performed, more long-term cell culture experiments were not reported, nor was the global ligand density present at the surface controlled.

3.3.2 Multivalent Integrin-binding Ligands Enhance Tissue Healing and Implant Integration *in vivo*

Petrie et al. also produced multivalent protein chimeras using transfected *E. Coli*.^[100] These protein chimeras contained the 7th to 10th domain of type III fibronectin, a 21 nm long flexible linker group derived from tenascin, and a coiled-coil domain that enabled complexation of the protein chimeras into monomers, dimers, tetramers, and pentamers (**Figure 16**). These multimers were then covalently immobilized to medical grade titanium surfaces that were passivated with a PEG layer.^[100]

In vitro, the surfaces were used as a substrate for MSC culture under osteogenic conditions.^[100] Surfaces presenting the trimeric and pentameric peptide exhibited twice as much integrin binding as the monomeric and dimeric surfaces. No difference in integrin binding was observed between the trimeric and pentameric surfaces, indicating a threshold response and not a monotonic increase with valency. Integrin signalling was also assessed through FAK phosphorylation studies, and it was found that surfaces functionalized with pentamers resulted in increased phosphorylation, again supporting the idea of a valency-dependent threshold effect. Additionally, cells cultured on trimeric and pentameric interfaces showed significantly more osteogenesis as assessed through an increase in alkaline phosphatase activity and calcium deposition.^[100]

In vivo, titanium rods functionalized with the multivalent ligands were implanted into tibia defects in a rat model designed to mimic dental and orthopedic clinical procedures.^[100] No evidence of fibrous encapsulation or chronic inflammation was observed for any groups. However, the researchers observed a 50% increase in bone-implant contact area for trimer-

and pentamer-functionalized materials compared to monomer- and dimer-functionalized surfaces and a 75% increase over unmodified titanium implants (the current clinical standard). Furthermore, through pullout tests, the trimer- and pentamer-functionalized surfaces exhibited a 250% increase in fixation compared to other functionalized surfaces and a 400% increase compared to bare titanium.^[100] These results provide the most clear support for the use of multivalent ligands in the development of future healthcare materials intended for *in vivo* use.

3.3.3 Recombinant Elastin-like Protein

Benitez, et al. also used recombinant protein expression to generate biomaterial substrates functionalized with nanoclusters of ligands.^[101] Specifically, the researchers utilized a recombinantly expressed elastin-like protein. This protein lacks intrinsic cell adhesive capacity, but can be engineered to contain cell adhesive groups, in this case the RGD peptide sequence. The researchers produced a recombinant protein that contained the cell adhesive RGD group and protein that contained the non-adhesive RDG group. These two proteins were then blended together in various ratios to control global and local ligand density (**Figure 17**). Another distinct feature of this research is that instead of producing planar cell culture surfaces, these materials were electrospun in order to produce fibrous mats. After electrospinning these protein scaffolds were crosslinked with glutaraldehyde to produce water-stable materials. Using this approach, the researchers were able to produce surfaces with a far wider range of ligand concentrations than previous techniques. Local ligand density varied from 0 to 122,000 ligands/ μm^2 and global ligand density from 0 to 71,000 ligands/ μm^2 .^[101]

In vitro cell culture experiments with HUVECs enabled the researchers to make several key observations. It is well established that when global ligand densities are too low, insufficient integrin binding occurs due to poor availability. Conversely, when the global density is too high most integrins can bind ligand while maintaining a random distribution, thus preventing clustering. The researchers identified that HUVECs on clustered surfaces performed best when the global ligand densities was approximately half of the saturation point for ligand-integrin interactions (approximately 12,000 RGD/ μm^2 for HUVECs).^[101] At these conditions, the cells exhibited increased cell proliferation, focal adhesion number and focal adhesion kinase expression. Additionally, at excessively high local ligand density (122,000 RGD/ μm^2), cell division, focal adhesion number, and focal adhesion kinase expression were significantly decreased; likely due to steric overcrowding of ligands.^[101]

4. Emerging Themes from Ligand Clustering Technology

4.1. Biology Knowledge

From a biological perspective, these studies have clearly illustrated the importance of integrin clustering in promoting a wide variety of cellular behaviours including adhesion, morphology, gene expression, proliferation rate, adhesion strength, and cellular differentiation. Additionally, both the local and global concentrations of ligands are critical mediators of these cellular functions, and there are optimum values of ligand density on both length scales. At an individual cluster level, Arnold, et al. studied focal adhesion formation on surfaces with as few as 6 ligands per island, and found that this local density is sufficient to achieve the desirable cellular behaviours for fibroblasts.^[95] Similarly, Petrie, et al. studied surfaces functionalized with 2 – 5 ligands per island, and it was determined that surfaces with 4 and 5 ligands per island were sufficient to improve cellular behaviour of MSCs *in vitro* and

biomedical device integration *in vivo*. For local densities below these levels, the maximal cell response was not observed, indicating that local densities of 4 – 6 ligands per island are required.^[100] From a biological perspective, this is an interesting discovery as focal adhesions can reach 500 nm in size and contain thousands of individual protein molecules, while the formation of these large and complex adhesions are nucleated by the clustering of relatively few ligands. As illustrated *in silico* by Brinkerhoff and Linderman, ligand clustering acts cooperatively with the natural propensity of integrins to dimerize through fast-forming and weak interactions enabling the aggregation of larger structures that act cooperatively in the formation of stable adhesion complexes.^[65]

In addition to the number of ligands per island, these studies have provided insight into the optimum spacing of ligands within an island. If the separation distance between ligands is too small, steric hindrance occurs, and cellular adhesion is inhibited.^[101] Conversely, if ligand spacing is too large, focal adhesions are unable to form and critical parameters such as cell adhesion and adhesion strength are compromised.^[80-84] Interestingly, this critical spacing between ligands has been shown to vary between cell types. For osteoblasts, melanocytes, and fibroblasts, a spacing of approximately 58 nm was required to enable focal adhesion formation, while for hematopoietic stem cells, a critical spacing of approximately 32 nm was identified.^[79, 82] In either scenario, advanced materials fabrication techniques are required in order to enable the appropriate nano-scale spacing of adhesive ligands.

In addition to the local density of ligands, the global density of ligands is also a critical parameter. For instance, it has long been known that there is a saturation point of ligands at the surface in order to maximize cell adhesion.^[25] Additionally, there is a biphasic trend

between ligand density and migration speed where too few ligands leads to slow cell migration due to poor cell/substrate interactions, too many ligands leads to slow cell migration due to an overabundance of cell/substrate interactions, and there is thus a maximum in migration at intermediate ligand densities.^[102] These studies have also increased understanding of the optimal global surface density of ligands and the optimal spacing between islands of ligands. For instance, it was illustrated that HUVECs on clustered surfaces perform best when the global ligand density was approximately half of the saturation point for ligand-integrin interactions (approximately 12,000 RGD/ μm^2).^[101] However, these experiments have not been performed using different cell types, limiting the conclusions that can be drawn from these data. Additionally, the distance between islands of ligands was illustrated to influence cell proliferation and differentiation capacity. Despite the general consensus that both global and local ligand presentation is critical in mediating cell function, there are discrepancies in the data. Specifically, as the lateral spacing between ligands increases, osteogenic differentiation of MSCs was found to decrease and adipogenic differentiation was found to increase in one study^[76], while greater lateral spacing between ligands was found to increase both osteogenic and adipogenic differentiation in another study.^[93] These results illustrate the importance of ligand clustering and provide general design guidelines in terms of how the spacing and density of ligands regulate cell behaviors. However, we still possess incomplete knowledge on how these parameters will influence the behavior of a given cell type, illustrating that optimization at multiple size scales is critical when designing a biomaterial interface. Additionally, other parameters such as ligand type are also likely important, yet this has not been thoroughly explored in a multivalent format.

Perhaps the most compelling data presented in this review is the improved *in vivo* performance of biomaterials and biomedical devices that are functionalized with multivalent integrin binding ligands. Suboptimal angiogenesis of tissue scaffolds is a longstanding problem that is limiting progress in the tissue engineering field, and the data reviewed in this article supports the idea that biomaterials functionalized with clustered ligands may play an important role in addressing this longstanding challenge.^[68] Additionally, the superior osteointegration and tissue healing observed by titanium implants that were functionalized with multivalent integrin binding ligands further supports the use of these materials in the fields of tissue engineering, regenerative medicine, and biomedical device design.^[100]

Interestingly, the first manuscripts describing the importance of clustering integrins on a biomaterial surface were published in the early 2000s.^[49] While generating biomaterials functionalized with nano-scale clusters of integrin binding ligands remains an active area of research,^[68, 101] it is not a technique that is widely adopted by the broader biomaterials and tissue engineering community, despite the clear benefits. One major goal of this review article is to raise awareness of this technology, so that it will become more widely explored and utilized in development of next generation biomaterials.

4.2. Materials Science

From a materials science point of view, several distinct methods of producing biomaterials with nano-clusters of integrin-binding ligands have been produced. Some are based on blending strategies and exploit the nanometer scale of single polymer molecules or nanoparticles, others rely on bottom up nanolithography techniques, and others still utilize protein-engineering methodologies. However, despite the method of production, these

studies clearly show that ligand clustering is an additional handle for biomaterials innovation.

All of these technologies have distinct advantages and disadvantages relating to ease of synthesis and fabrication, cost, and control and assessment of the interface (**Table 3**). The authors feel that certain techniques are more promising platforms for future development. Specifically, the NIL approach provides the most flexible platform for studying how basic biological phenomena are related to exact spacing of ligands. The authors prefer this method compared to micelle nanolithography, as the micelle approach is currently limited to a hexagonal packing of nanoparticles while the NIL approach enables greater control of the ligand distribution within a given ligand island, although this potential has not yet been fully explored.

Unfortunately, the lithography technologies are limited by the size, scale, shape, and material composition of the substrates. Additionally, the utilization of (gold) nanoparticles potentiates undesirable ramifications including toxicity if used *in vivo*.^[103] For larger scale applications such as the fabrication of biomedical devices and tissue scaffolds, the polymer blending strategies appear the most promising as they utilize standard and readily available chemistries, the polymers can be fabricated into complex and three dimensional shapes via established scaffold fabrication techniques or coated onto the surface of implants, and they do not rely on complex protein engineering technologies. Although these blending techniques do not provide the granular control of ligand presentation at the interface, the extensive body of literature presented in this review illustrates that these surfaces are sufficient to promote ligand occupancy and clustering, and thus achieve improved cellular interactions.

From an economic point of view, the use of biomaterials functionalized with clusters of integrin binding ligands is also advantageous. When synthesizing biofunctionalized materials, the peptide ligands or recombinant protein fragments are often the most expensive component due to the laborious, time consuming, and specialized techniques required for their production and purification. Therefore, maximizing the biological impact of the ligand is desirable from the point of view of production cost. Glass, et al. illustrated that cells adherent to biomaterials functionalized with islands of ligands exhibited the same behaviours as surfaces that were homologously functionalized with peptide at the same lateral spacing, despite the fact that the homologously functionalized surface contained ~6-fold more peptide.^[94] This means that the surfaces functionalized with nanoclusters of ligands evoked the same biological behaviour from adherent cells as was observed on a surface that contained a much larger quantity of ligand. Thus, this technology may provide a path towards significantly reducing the cost of functionalized biomaterials.

5. Future Directions

The authors see several directions for future research related to nanoclustering of integrin binding ligands that would lead to improved knowledge of biology and improved performance of biomedical devices. The first logical steps revolve around expanding the palette of ligands and cells that have been studied. Thus far, the impact of multivalent ligands has only been explored on relatively few cell types including fibroblasts, preosteoblasts, myoblasts, HUVECs, MSCs, HSCs, and cancer cells. However, the ability to regulate key processes of these cells including proliferation, gene expression, and differentiation warrants the study of how ligand clustering impacts other cell types. Additionally, of the numerous number of integrin binding ligands that have been identified, only the RGD ligand has been

thoroughly explored in a clustered format. Different ligand types can result in drastically different cellular behaviours.^[68, 75, 104, 105] As such, assessing the impact of nanoclustering on a wider variety of integrin binding ligands is of interest. Furthermore, only integrin binding ligands have been explored. While integrins are the primary receptor family for cell/ECM interactions, they are not the only family of receptors that connects the cell to the ECM. Additionally, clustering is also critical for the biological performance of other receptor types such as the syndecan receptors.^[106-108] The authors propose that advanced biomaterials can be generated by exploring ligands for other receptor types in a multivalent format.^[109-111]

Ligand multivalency may also play a role in the development of advanced materials for *ex vivo* cell expansion and biomedical implants. Recent research has shown that decellularized extracellular matrix materials (dECMs) are useful for maintaining the phenotype of cells during large-scale expansion.^[112-114] However, such dECM materials are limited in availability, are often isolated from allogenic or xenogenic sources, and are difficult to sterilize.^[115] Therefore, developing synthetic mimics to these materials is an area of great interest. The research described in this review has illustrated that ligand density and patterning regulates key cell parameters including proliferation and differentiation. Therefore, we posit that ligand multivalency will play an important role in the development of next generation synthetic healthcare materials for xeno-free cell expansion.

The impact of ligand multivalency in the field of cellular biomechanics has also been largely unexplored. Focal adhesions act as signalling nexuses for cells and the mechanical forces they experience. As described in this review, initial work has been performed to assess how multivalent ligand presentation interacts with substrate stiffness to regulate cellular

behaviors.^[61, 92, 93] However, improved understanding in this area is needed. Specifically, the range of substrate moduli explored by Hsiong, et al. was relatively narrow (20 – 110 kPa).^[61] Coupling multivalent ligand presentation with a wider range of substrate stiffnesses could lead to more biomimetic *in vitro* assays for exploring the impact of substrate mechanics on cell types. The literature reported herein has already illustrated the utility of multivalent ligands in developing *ex vivo* models of disease states such as cancer metastasis.^[88] Coupling such materials with substrate mechanics could provide an *in vitro* platform to more faithfully model several challenging pathologies (e.g. liver fibrosis) which is hallmarked by stiffening of the ECM.^[116] Beyond substrate mechanical properties, integrins are also critical in the response of cells to applied mechanical forces.^[117, 118] As such, multivalent ligand technology could have substantial impact in the field of cellular biomechanics and its applications in tissue engineering. Many scaffolds are seeded with cells and matured in bioreactors with applied stresses,^[119, 120] a step that is critical for the development of the neo-tissue. The authors predict that coupling multivalent ligands with mechanical loading will increase the cellular response to these mechanical stressors. Beyond advancing fundamental mechanobiology knowledge, this could lead to improved design of tissue engineering scaffolds.

Clinically, we also envision this technology improving the performance of biomedical devices. The work presented in this review has already illustrated the ability of ligand clustering to improve the vascularization^[68] and osteogenic integration^[100] of materials *in vivo*. Taken together, the *in vitro* and *in vivo* data illustrate that advanced materials can be fabricated utilizing the design principles and knowledge generated from these studies to improve the performance of future biomedical devices and tissue engineering constructs. However, the design of next generation biomaterials for *in vivo* applications has additional

constraints. First, most of the studies reviewed in this article have focused on the utilization of multivalent ligands in a 2D planar geometry. However, most tissues have a complex and three-dimensional shape. To the authors' knowledge, only two studies have explored the impact of multivalent ligands on complex 3D structures, meaning there is great scope for assessing the impact of assessing the interplay between multivalent ligands and a three dimensional cell growth environment.^[57, 101] Generating novel biomaterials suitable for scaffold production through techniques such as 3D printing or electrospinning or injectable materials based on thermoreversible or UV curable gelation that display ligands in a multivalent format will be of upmost interest.^[121-123] Additionally, other constraints such as the host reaction to the material – including protein adsorption/denaturing, fibrous encapsulation, chronic inflammation, and blood coagulation – must be considered. For these reasons, the authors feel that the polymer blending strategies are most suitable for *in vivo* use. This technique enables the properties of the bulk polymer to be engineered. Specifically, the polymer can be designed with non-fouling properties (such as the PEG-based or alginate-based materials reviewed herein). These materials prevent the deposition of biomolecules from the biological milieu, and as such are generally well tolerated by the body.^[124, 125] For instance, the article by Petrie et al. coated titanium implants with a PEG-based material functionalized with multivalent ligands. The researchers did not observe the development of a fibrous capsule or chronic inflammation.^[100] However, there is growing evidence that illustrates that PEG may undergo degradation *in vivo*.^[126-128] As such, the *in vivo* study of ligand multivalency on next generation non-fouling materials such as zwitterionic materials or polyoxazolines is required.^[20-24]

Acknowledgements

The authors would like to thank the Research Training Program (RTP), the Endeavor IPRS, and the Australian Postgraduate Awards (APA) for providing financial support to this project.

References

- [1] B. G. Keselowsky, D. M. Collard, A. J. García, *Biomaterials* **2004**, *25*, 5947.
- [2] J. Vitte, A. Benoliel, A. Pierres, P. Bongrand, *Eur Cell Mater* **2004**, *7*, 52.
- [3] D. E. Heath, J. J. Lannutti, S. L. Cooper, *J. Biomed. Mater. Res. A* **2010**, *94*, 1195.
- [4] A. J. Engler, S. Sen, H. L. Sweeney, D. E. Discher, *Cell* **2006**, *126*, 677.
- [5] D. Khatayevich, M. Gungormus, H. Yazici, C. So, S. Cetinel, H. Ma, A. Jen, C. Tamerler, M. Sarikaya, *Acta Biomater.* **2010**, *6*, 4634.
- [6] U. Hersel, C. Dahmen, H. Kessler, *Biomaterials* **2003**, *24*, 4385.
- [7] A. N. Veleva, D. E. Heath, S. L. Cooper, C. Patterson, *Biomaterials* **2008**, *29*, 3656.
- [8] J. D. Humphries, A. Byron, M. J. Humphries, *J. Cell. Sci.* **2006**, *119*, 3901.
- [9] R. O. Hynes, *Cell* **2002**, *110*, 673.
- [10] S. M. Cutler, A. J. García, *Biomaterials* **2003**, *24*, 1759.
- [11] B. Geiger, A. Bershadsky, R. Pankov, K. M. Yamada, *Nat. Rev. Mol. Cell Biol.* **2001**, *2*, 793.
- [12] N. Strohmeyer, M. Bharadwaj, M. Costell, R. Fässler, D. J. Müller, *Nat. Mater.* **2017**.
- [13] C. D. Reyes, A. J. García, *J. Biomed. Mater. Res. A* **2003**, *65*, 511.
- [14] M. Nomizu, B. S. Weeks, C. A. Weston, W. H. Kim, H. K. Kleinman, Y. Yamada, *FEBS Lett.* **1995**, *365*, 227.
- [15] X. Wang, D. E. Heath, S. L. Cooper, *J. Biomed. Mater. Res. A* **2012**, *100*, 794.
- [16] R. Cherny, M. A. Honan, P. Thiagarajan, *J. Biol. Chem.* **1993**, *268*, 9725.
- [17] K. S. Masters, K. S. Anseth, *Adv. Chem. Eng.* **2004**, *29*, 7.
- [18] E. F. Plow, T. A. Haas, L. Zhang, J. Loftus, J. W. Smith, *J. Biol. Chem.* **2000**, *275*, 21785.
- [19] D. E. Heath, S. L. Cooper, *J Biomater Sci Polym Ed* **2017**, *1*.
- [20] S. Chen, L. Li, C. Zhao, J. Zheng, *Polymer* **2010**, *51*, 5283.
- [21] T. Ueda, H. Oshida, K. Kurita, K. Ishihara, N. Nakabayashi, *Polym. J.* **1992**, *24*, 1259.
- [22] D. E. Heath, S. L. Cooper, *Acta Biomater.* **2012**, *8*, 2899.
- [23] D. E. Heath, S. L. Cooper, *J. Biomed. Mater. Res. A* **2010**, *94*, 1294.
- [24] M. Morra, C. Cassineli, *J Biomater Sci Polym Ed* **1999**, *10*, 1107.
- [25] S. P. Massia, J. A. Hubbell, *J. Cell Biol.* **1991**, *114*, 1089.
- [26] S. Miyamoto, S. K. Akiyama, K. M. Yamada, *Science* **1995**, *267*, 883.
- [27] I. Aukhil, P. Joshi, Y. Yan, H. P. Erickson, *J. Biol. Chem.* **1993**, *268*, 2542.
- [28] R. O. Hynes, K. M. Yamada, *J. Cell Biol.* **1982**, *95*, 369.
- [29] D. A. Calderwood, S. J. Shattil, M. H. Ginsberg, *J. Biol. Chem.* **2000**, *275*, 22607.
- [30] T. A. Springer, J.-H. Wang, *Adv. Protein Chem.* **2004**, *68*, 29.
- [31] P. Kanchanawong, G. Shtengel, A. M. Pasapera, E. B. Ramko, M. W. Davidson, H. F. Hess, C. M. Waterman, *Nature* **2010**, *468*, 580.
- [32] H. Lodish, A. Berk, P. Matsudaira, A. C. Kaise, M. Krieger, J. E. Darnell, P. M. Scott, L. Zipursky, *Molecular cell biology*, Scientific American Books New York, **2003**.
- [33] C. Wu, *Histol. Histopathol.* **1997**, *12*, 233.
- [34] S. J. Shattil, *Thromb. Haemost.* **1999**, *82*, 318.
- [35] M. L. Gardel, I. C. Schneider, Y. Aratyn-Schaus, C. M. Waterman, *Annu. Rev. Cell Dev. Biol.* **2010**, *26*, 315.
- [36] L. Kornberg, H. S. Earp, J. T. Parsons, M. Schaller, R. L. Juliano, *J. Biol. Chem.* **1992**, *267*, 23439.
- [37] K. R. Legate, S. A. Wickström, R. Fässler, *Genes Dev.* **2009**, *23*, 397.
- [38] A. L. Berrier, K. M. Yamada, *J. Cell. Physio.* **2007**, *213*, 565.
- [39] M. A. Wozniak, K. Modzelewska, L. Kwong, P. J. Keely, *Biochim. Biophys. Acta* **2004**, *1692*, 103.
- [40] S. K. Mitra, D. A. Hanson, D. D. Schlaepfer, *Nat. Rev. Mol. Cell Biol.* **2005**, *6*, 56.

- [41] D. S. Harburger, D. A. Calderwood, *J. Cell. Sci.* **2009**, *122*, 159.
- [42] B. Wehrle-Haller, *Curr. Opin. Cell Biol.* **2012**, *24*, 569.
- [43] D. R. Critchley, A. R. Gingras, *J. Cell. Sci.* **2008**, *121*, 1345.
- [44] E. Ruoslahti, J. C. Reed, *Cell* **1994**, *77*, 477.
- [45] P. Moreno-Layseca, C. H. Streuli, *Matrix Biol.* **2014**, *34*, 144.
- [46] M. A. Schwartz, R. K. Assoian, *J. Cell. Sci.* **2001**, *114*, 2553.
- [47] V. J. Thannickal, D. Y. Lee, E. S. White, Z. Cui, J. M. Larios, R. Chacon, J. C. Horowitz, R. M. Day, P. E. Thomas, *J. Biol. Chem.* **2003**, *278*, 12384.
- [48] M. J. Gómez-Lamarca, L. Cobreros-Reguera, B. Ibáñez-Jiménez, I. M. Palacios, M. D. Martín-Bermudo, *J. Cell Sci.* **2014**, *127*, 4667.
- [49] G. Maheshwari, G. Brown, D. A. Lauffenburger, A. Wells, L. G. Griffith, *J. Cell. Sci.* **2000**, *113*, 1677.
- [50] D. J. Irvine, A. M. Mayes, L. G. Griffith, *Biomacromolecules* **2001**, *2*, 85.
- [51] L. Y. Koo, D. J. Irvine, A. M. Mayes, D. A. Lauffenburger, L. G. Griffith, *J. Cell. Sci.* **2002**, *115*, 1423.
- [52] W. A. Kuhlman, E. A. Olivetti, L. G. Griffith, A. M. Mayes, *Macromolecules* **2006**, *39*, 5122.
- [53] W. Kuhlman, I. Taniguchi, L. G. Griffith, A. M. Mayes, *Biomacromolecules* **2007**, *8*, 3206.
- [54] D. J. Irvine, A.-V. G. Ruzette, A. M. Mayes, L. G. Griffith, *Biomacromolecules* **2001**, *2*, 545.
- [55] D. E. Heath, *Macromol. Chem. Phys.* **2017**, *218*.
- [56] F. Karimi, T. G. McKenzie, A. J. O'Connor, G. G. Qiao, D. E. Heath, *J. Mater. Chem. B* **2017**, *5*, 5942.
- [57] K. Y. Lee, E. Alsberg, S. Hsiong, W. Comisar, J. Linderman, R. Ziff, D. Mooney, *Nano Lett.* **2004**, *4*, 1501.
- [58] W. A. Comisar, N. H. Kazmers, D. J. Mooney, J. J. Linderman, *Biomaterials* **2007**, *28*, 4409.
- [59] M.-S. Bae, K. Y. Lee, Y. J. Park, D. J. Mooney, *Macromol Res.* **2007**, *15*, 469.
- [60] T. Boonthuekul, H.-J. Kong, S. X. Hsiong, Y.-C. Huang, L. Mahadevan, H. Vandenberg, D. J. Mooney, *Faraday Discuss.* **2008**, *139*, 53.
- [61] S. X. Hsiong, P. Carampin, H. J. Kong, K. Y. Lee, D. J. Mooney, *J. Biomed. Mater. Res. A* **2008**, *85*, 145.
- [62] H. J. Kong, S. Hsiong, D. J. Mooney, *Nano Lett.* **2007**, *7*, 161.
- [63] W. A. Comisar, S. X. Hsiong, H.-J. Kong, D. J. Mooney, J. J. Linderman, *Biomaterials* **2006**, *27*, 2322.
- [64] W. Comisar, D. Mooney, J. Linderman, *J. Theor. Biol.* **2011**, *274*, 120.
- [65] C. J. Brinkerhoff, J. J. Linderman, *Tissue Eng.* **2005**, *11*, 865.
- [66] E. Laplantine, P. Maurer, L. Vallar, J. Eble, M. Paulsson, P. Bruckner, N. Kieffer, M. Aumailley, *Biol. Cell* **2002**, *94*, 375.
- [67] S. Myou, X. Zhu, E. Boetticher, Y. Qin, S. Myo, A. Meliton, A. Lambertino, N. M. Munoz, K. J. Hamann, A. R. Leff, *Immunology* **2002**, *107*, 77.
- [68] B. Wang, W. Wang, Y. Yu, Y. Zhang, J. Zhang, Z. Yuan, *Colloids Surf. B: Biointerfaces* **2017**, *154*, 383.
- [69] S. P. Massia, J. A. Hubbell, *J. Biol. Chem.* **1992**, *267*, 14019.
- [70] Y. Ji, Y. Wei, X. Liu, J. Wang, K. Ren, J. Ji, *J. Biomed. Mater. Res. A* **2012**, *100*, 1387.
- [71] Y. Wei, Y. Ji, L.-L. Xiao, Q.-k. Lin, J.-p. Xu, K.-f. Ren, J. Ji, *Biomaterials* **2013**, *34*, 2588.
- [72] P. A. George, J. J. Cooper-White, *Eur. Polym. J.* **2009**, *45*, 1065.
- [73] P. A. George, B. C. Donose, J. J. Cooper-White, *Biomaterials* **2009**, *30*, 2449.
- [74] P. A. George, M. R. Doran, T. I. Croll, T. P. Munro, J. J. Cooper-White, *Biomaterials* **2009**, *30*, 4732.
- [75] H. Li, J. Frith, J. J. Cooper-White, *Biomacromolecules* **2013**, *15*, 43.
- [76] J. E. Frith, R. J. Mills, J. J. Cooper-White, *J. Cell. Sci.* **2012**, *125*, 317.
- [77] K. L. Killops, N. Gupta, M. D. Dimitriou, N. A. Lynd, H. Jung, H. Tran, J. Bang, L. M. Campos, *ACS Macro Lett.* **2012**, *1*, 758.

- [78] J. P. Spatz, S. Mössmer, C. Hartmann, M. Möller, T. Herzog, M. Krieger, H.-G. Boyen, P. Ziemann, B. Kabius, *Langmuir* **2000**, *16*, 407.
- [79] M. Arnold, E. A. Cavalcanti-Adam, R. Glass, J. Blümmel, W. Eck, M. Kantelehner, H. Kessler, J. P. Spatz, *ChemPhysChem* **2004**, *5*, 383.
- [80] E. A. Cavalcanti-Adam, A. Micoulet, J. Blümmel, J. Auernheimer, H. Kessler, J. P. Spatz, *Eur. J. Cell Biol.* **2006**, *85*, 219.
- [81] E. A. Cavalcanti-Adam, T. Volberg, A. Micoulet, H. Kessler, B. Geiger, J. P. Spatz, *Biophys. J.* **2007**, *92*, 2964.
- [82] E. Altmann, C. A. Muth, G. Klein, J. P. Spatz, C. Lee-Thedieck, *Biomaterials* **2012**, *33*, 3107.
- [83] C. Selhuber-Unkel, M. López-García, H. Kessler, J. P. Spatz, *Biophys. J.* **2008**, *95*, 5424.
- [84] C. Selhuber-Unkel, T. Erdmann, M. Lopez-Garcia, H. Kessler, U. Schwarz, J. Spatz, *Biophys. J.* **2010**, *98*, 543.
- [85] F. Rechenmacher, S. Neubauer, J. Polleux, C. Mas-Moruno, M. De Simone, E. A. Cavalcanti-Adam, J. P. Spatz, R. Fässler, H. Kessler, *Angew. Chem. Int. Ed.* **2013**, *52*, 1572.
- [86] V. Schaufli, H. Czichos-Medda, V. Hirschfeld-Warneken, S. Neubauer, F. Rechenmacher, R. Medda, H. Kessler, B. Geiger, J. P. Spatz, E. A. Cavalcanti-Adam, *Cell Adhes. Migr.* **2016**, *10*, 505.
- [87] Y. Shimizu, H. Boehm, K. Yamaguchi, J. P. Spatz, J. Nakanishi, *PLOS One* **2014**, *9*, e91875.
- [88] K. Amschler, L. Erpenbeck, S. Kruss, M. P. Schön, *ACS nano* **2014**, *8*, 9113.
- [89] J. Huang, S. V. Grater, F. Corbellini, S. Rinck, E. Bock, R. Kemkemer, H. Kessler, J. Ding, J. P. Spatz, *Nano Lett.* **2009**, *9*, 1111.
- [90] M. Arnold, V. C. Hirschfeld-Warneken, T. Lohmüller, P. Heil, J. Blümmel, E. A. Cavalcanti-Adam, M. López-García, P. Walther, H. Kessler, B. Geiger, *Nano Lett.* **2008**, *8*, 2063.
- [91] V. C. Hirschfeld-Warneken, M. Arnold, A. Cavalcanti-Adam, M. López-García, H. Kessler, J. P. Spatz, *Eur. J. Cell Biol.* **2008**, *87*, 743.
- [92] S. V. Graeter, J. Huang, N. Perschmann, M. López-García, H. Kessler, J. Ding, J. P. Spatz, *Nano Lett.* **2007**, *7*, 1413.
- [93] X. Wang, C. Yan, K. Ye, Y. He, Z. Li, J. Ding, *Biomaterials* **2013**, *34*, 2865.
- [94] R. Glass, M. Möller, J. P. Spatz, *Nanotechnology* **2003**, *14*, 1153.
- [95] M. Arnold, M. Schwieder, J. Blümmel, E. A. Cavalcanti-Adam, M. López-García, H. Kessler, B. Geiger, J. P. Spatz, *Soft Matter* **2009**, *5*, 72.
- [96] M. Schwartzman, K. Nguyen, M. Palma, J. Abramson, J. Sable, J. Hone, M. Sheetz, S. Wind, *J. Vac. Sci. Technol. B* **2009**, *27*, 61.
- [97] M. Schwartzman, M. Palma, J. Sable, J. Abramson, X. Hu, M. P. Sheetz, S. J. Wind, *Nano Lett.* **2011**, *11*, 1306.
- [98] M. Kreiner, Z. Li, J. Beattie, S. Kelly, H. Mardon, C. Van Der Walle, *Protein Eng. Des. Sel.* **2008**, *21*, 553.
- [99] N. A. Hotchin, A. G. Kidd, H. Altroff, H. J. Mardon, *J. Cell Sci.* **1999**, *112*, 2937.
- [100] T. A. Petrie, J. E. Raynor, D. W. Dumbauld, T. T. Lee, S. Jagtap, K. L. Templeman, D. M. Collard, A. J. García, *Sci. Transl. Med.* **2010**, *2*, 45ra60.
- [101] P. L. Benítez, S. Mascharak, A. C. Proctor, S. C. Heilshorn, *Integr. Biol.* **2016**, *8*, 50.
- [102] S. P. Palecek, J. C. Loftus, M. H. Ginsberg, D. A. Lauffenburger, A. F. Horwitz, *Nature* **1997**, *385*, 537.
- [103] Y.-S. Chen, Y.-C. Hung, I. Liao, G. S. Huang, *Nanoscale Res. Lett.* **2009**, *4*, 858.
- [104] Y. Lei, M. Rémy, C. Labrugère, M.-C. Durrieu, *J. Mater. Sci. Mater. Med* **2012**, *23*, 2761.
- [105] C. C. Larsen, F. Kligman, C. Tang, K. Kottke-Marchant, R. E. Marchant, *Biomaterials* **2007**, *28*, 3537.
- [106] S. M. Jay, E. Kurtagic, L. M. Alvarez, S. de Picciotto, E. Sanchez, J. F. Hawkins, R. N. Prince, Y. Guerrero, C. L. Treasure, R. T. Lee, *J. Biol. Chem.* **2011**, *286*, 27729.
- [107] L. L. Kiessling, J. E. Gestwicki, L. E. Strong, *Angew. Chem. Int. Ed.* **2006**, *45*, 2348.
- [108] S. Bhatia, M. Dimde, R. Haag, *Med. Chem. Commun.* **2014**, *5*, 862.
- [109] J. Brasch, O. J. Harrison, B. Honig, L. Shapiro, *Trends Cell Biol.* **2012**, *22*, 299.

- [110] G. Bendas, L. Borsig, *Int. J. Cell Biol.* **2012**, 2012.
- [111] S.-H. Kim, J. Turnbull, S. Guimond, *J. Endocrinol.* **2011**, 209, 139.
- [112] A. Shakouri-Motlagh, A. J. O'Connor, S. P. Brennecke, B. Kalionis, D. E. Heath, *Acta Biomater.* **2017**.
- [113] G. D. Kusuma, S. P. Brennecke, A. J. O'Connor, B. Kalionis, D. E. Heath, *PLOS One* **2017**, 12, e0171488.
- [114] N. Rao, G. Agmon, M. T. Tierney, J. L. Ungerleider, R. L. Braden, A. Sacco, K. L. Christman, *ACS nano* **2017**, 11, 3851.
- [115] T. Hoshiba, H. Lu, N. Kawazoe, G. Chen, *Expert Opin. Biol. Ther.* **2010**, 10, 1717.
- [116] R. G. Wells, *J. Clin. Gastroenterol* **2005**, 39, S158.
- [117] A. Katsumi, A. W. Orr, E. Tzima, M. A. Schwartz, *J. Biol. Chem.* **2004**, 279, 12001.
- [118] M. A. Schwartz, *CSH Perspect Biol.* **2010**, 2, a005066.
- [119] N. Wang, S. Grad, M. J. Stoddart, P. Niemeyer, N. P. Südkamp, J. Pestka, M. Alini, J. Chen, G. M. Salzmann, *Cartilage* **2013**, 4, 165.
- [120] C. Meinert, K. Schrobback, D. W. Hutmacher, T. J. Klein, *Sci. Rep.* **2017**, 7, 16997.
- [121] Z. Zhang, Y. Lai, L. Yu, J. Ding, *Biomaterials* **2010**, 31, 7873.
- [122] A. Sivashanmugam, R. A. Kumar, M. V. Priya, S. V. Nair, R. Jayakumar, *Eur. Polym. J.* **2015**, 72, 543.
- [123] D. E. Heath, C. Kobe, D. Jones, N. I. Moldovan, S. L. Cooper, *Tissue Eng. Part A.* **2012**, 19, 79.
- [124] A. W. Bridges, A. J. García, *J. Diabetes Sci. Technol.* **2008**, 2, 984.
- [125] A. Vishwakarma, N. S. Bhise, M. B. Evangelista, J. Rouwkema, M. R. Dokmeci, A. M. Ghaemmaghami, N. E. Vrana, A. Khademhosseini, *Trends Biotechnol.* **2016**, 34, 470.
- [126] M. Shen, L. Martinson, M. S. Wagner, D. G. Castner, B. D. Ratner, T. A. Horbett, *J Biomater Sci Polym Ed* **2002**, 13, 367.
- [127] L. Li, S. Chen, S. Jiang, *J Biomater Sci Polym Ed* **2007**, 18, 1415.
- [128] E. Ostuni, R. G. Chapman, R. E. Holmlin, S. Takayama, G. M. Whitesides, *Langmuir* **2001**, 17, 5605.
- [129] J. Deng, C. Zhao, J. P. Spatz, Q. Wei, *ACS nano* **2017**, 11, 8282.
- [130] X. Wang, S. Li, C. Yan, P. Liu, J. Ding, *Nano Lett.* **2015**, 15, 1457.
- [131] K. Ye, X. Wang, L. Cao, S. Li, Z. Li, L. Yu, J. Ding, *Nano Lett.* **2015**, 15, 4720.
- [132] Z. Li, B. Cao, X. Wang, K. Ye, S. Li, J. Ding, *J. Mater. Chem. B* **2015**, 3, 5197.
- [133] X. Wang, K. Ye, Z. Li, C. Yan, J. Ding, *Organogenesis* **2013**, 9, 280.
- [134] J. Huang, J. Ding, *Soft Matter* **2010**, 6, 3395.
- [135] K. Ye, L. Cao, S. Li, L. Yu, J. Ding, *ACS Appl. Mater. Interfaces* **2015**, 8, 21903.
- [136] S. Li, X. Wang, B. Cao, K. Ye, Z. Li, J. Ding, *Nano Lett.* **2015**, 15, 7755.

Table 1. Comparison of substrate patterning for biomaterials functionalized with multivalent integrin binding ligands. Values are not available for cells that are blank.

Substrate	Average ligands per island (#)	Average ligand spacing within island (nm)	Average spacing between islands (nm)	Global ligand density (# / μm^2)	Ref
Blending techniques					

PEG star polymers	1 - 9		6 - 300	1,000 - 200,000	[49]
PMMA- <i>b</i> -POEM comb polymers	1.7 - 5.4	14 - 25	50 - 300	190 – 5,500	[50-54, 56]
Alginate hydrogels	1 - 25		36 - 168	3000 – 60,000	[57-62, 64]
Alginate hydrogels with gold nanoparticles					[68]
PS- <i>b</i> -PEO block copolymer	6		29-62	1,000 - 4,500	[72-77]
Nanolithography techniques					
Nanoparticle arrays via micelle nanolithography			20 - 250		[78-84, 86-95]
Nanoparticle arrays via nanoimprint lithography	2 - 7	50 - 100			[96, 97]
Biotechnology techniques					
Protein chimeras	1 - 4				[98]
Protein chimeras	1 - 5	10 -50		903	[100]
Recombinant elastin-like protein				0 – 71,000	[101]

Table 2. Comparison of key biological responses to biomaterials functionalized with multivalent ligands.

Substrate	Ligands	Cell types	Key biological findings	Ref
Blending techniques				
PEG star polymers	Linear RGD	WT NR6 Fibroblasts	<ul style="list-style-type: none"> Clustered surfaces promote adhesion complex formation; Enable increased cellular 	[49]

			<p>migration speed;</p> <ul style="list-style-type: none"> Interact with growth factor signaling to synergistically increase cell migration speed; Improve adhesion strength of cells 	
PMMA-r- POEM comb polymers	Linear RGD, synKRGD	WT NR6 Fibroblast s	<ul style="list-style-type: none"> Clustered surfaces result in “reinforcement” of cell adhesive strength; Longer tethers between the ligand and polymer backbone enables faster assembly of adhesion complexes, cell adhesion, and cell spreading; These polymers can be blended with standard scaffolds materials (ex. PLLA) and impart non-fouling and bio-specific function 	[50-54]
	Linear RGD	HUVECs	<ul style="list-style-type: none"> Clustered surfaces improved HUVECs adhesion, migration, and proliferation rate at the highest local and global peptide density 	[56]
Alginate hydrogels	Linear RGD, cyclic RGD	MC3T3- E1 preosteob lasts, human bone marrow mesenchy mal stem cells	<ul style="list-style-type: none"> Nanoscale organization of ligands regulates adhesion, proliferation, and osteogenic differentiation; Influences FAK phosphorylation, cell spreading, and proliferation rate; Regulates nonviral gene delivery and expression; Nanoscale organization of ligand and substrate stiffness can be cooperatively tuned to promote 	[57, 58, 61, 62, 64]

			proliferation	
	Linear RGD	Fibroblasts	<ul style="list-style-type: none"> Nanoscale organization of ligands regulates adhesion and proliferation rate 	[59]
	Linear RGD, cyclic RGD	Myoblasts	<ul style="list-style-type: none"> Nanoscale presentation of ligands regulates proliferation rate 	[60]
Alginate hydrogels with gold nanoparticles	Linear REDV	HUVECs	<ul style="list-style-type: none"> Clustered surfaces increases HUVEC adhesion and support larger numbers of HUVECs after 7 days of culture; <i>In vivo</i>, gels with nanoclustered ligands promote angiogenesis 	[68]
PS-b-PEO block copolymer	Linear RGD, FNIII ₇₋₁₀	3T3 fibroblasts	<ul style="list-style-type: none"> Nanoscale organization of ligands regulates cell adhesion, focal adhesion formation, and morphology 	[73, 74, 77]
	Linear RGD, IKVAV	Bone marrow MSCs	<ul style="list-style-type: none"> Cell adhesion was not affected by ligand type; however, cell spreading was significantly greater on RGD-functionalized surfaces 	[75]
	Linear RGD	Bone marrow MSCs	<ul style="list-style-type: none"> Lateral spacing of ligands influences cell spreading, cytoskeletal organization, focal adhesion formation, and osteogenic differentiation 	[76]
Nanolithography techniques				

Nanoparticle arrays via micelle nanolithography	Cyclic RGD	REF52 fibroblasts, B16 melanocytes, and 3T3 fibroblasts	<ul style="list-style-type: none"> • Lateral spacing between ligands $\geq 73\text{nm}$ results in limited cell adhesion, spreading, actin filament formation, and focal adhesion formation; • Cell spreading is slower and migration is more erratic on surfaces with 108nm between ligands compared to 58nm; • Lateral spacing between ligands $\geq 90\text{nm}$ focal adhesion formation is inhibited and cell adhesion strength and stiffness of the cell body decreases; • Only 6 ligands per island are required to establish focal adhesions 	[79-81, 83, 84, 90, 92, 95]
		Hematopoietic stem cells	<ul style="list-style-type: none"> • Lateral spacing of ligands of 32nm results in a greater degree of lipid raft clustering compared to 58nm; 	[82]
		HeLa cells	<ul style="list-style-type: none"> • Cells lose cell-cell contacts when migrating on surfaces with lateral ligand spacing of 52nm, yet retain more cell-cell contacts on homogeneous surfaces 	[87]
		Melanoma cells	<ul style="list-style-type: none"> • Soluble integrin-directed antitumoral compounds may shift melanoma cells into a more permissive state and facilitate metastasis 	[88]
		MC3T3-E1 osteoblasts	<ul style="list-style-type: none"> • Disorder in ligand lateral spacing can improve cell adhesion and spreading; • Cells can sense $\sim 1\text{nm}$ changes in 	[79, 89-91, 129]

			ligand spacing, and this results in cell polarization and migration towards more closely spaced ligands	
		Bone marrow MSCs	<ul style="list-style-type: none"> Lateral spacing of ligands along with matrix stiffness and cell-cell interactions regulate multilineage differentiation potential of MSCs Larger lateral spacing between ligands was found to enhance maintenance of chondrogenic phenotype 	[93, 130-135] [136]
	$\alpha_5\beta_1$ - and $\alpha_v\beta_3$ - agonists	U2OS osteosarcoma cells	<ul style="list-style-type: none"> Activation of $\alpha_v\beta_3$ integrin is not essential for initial cell adhesion and spreading but is essential for formation of stable focal adhesions 	[86]
Nanoparticle arrays via nanoimprint lithography	Cyclic RGD	3T3 fibroblasts	<ul style="list-style-type: none"> 4 ligands per island was a critical threshold that must be met to facilitate cell spreading 	[96, 97]
Biotechnology techniques				
Protein chimeras	FNIII ₉₋₁₀	BHK fibroblasts	<ul style="list-style-type: none"> Ligand clustering increases cell spreading 	[98]
Protein chimeras	FNIII ₇₋₁₀	MSCs	<ul style="list-style-type: none"> Cells adherent to surfaces functionalized with islands containing ≥ 3 ligands showed significantly more integrin binding and osteogenic differentiation; Greater FAK phosphorylation was observed for cells adherent to surfaces functionalized with 	[100]

			<p>islands containing 5 ligands;</p> <ul style="list-style-type: none"> No difference in integrin binding was observed by cells on islands containing 3 or 5 ligands indicating a possible threshold of local density that must be reached; <i>In vivo</i>, implants functionalized with islands of 3 and 5 ligands showed significantly greater osteointegration in bone healing model 	
Recombinant elastin-like protein	Linear RGD	HUVECs	<ul style="list-style-type: none"> If appropriately clustered, cells exhibit similar proliferation, focal adhesion formation, and focal adhesion kinase expression as cells grown on random surfaces with much higher global ligand density If local ligand density is too high, ligands are unavailable for cell binding due to steric hindrance 	[101]

Table 3. Advantages and disadvantages of techniques used to produce biomaterials functionalized with multivalent ligands.

Substrate	Advantages	Disadvantages	Ref
Blending techniques			
PEG star polymers	<ul style="list-style-type: none"> Enables precise control over the size of nanoscale islands due to size of star polymer; Materials are 	<ul style="list-style-type: none"> Polymers are water soluble, requiring covalent immobilization to an interface; Some ligands may be unavailable for cell binding due to the orientation of the star 	[49]

	commercially available	polymer at the interface	
PMMA-r-POEM comb polymers	<ul style="list-style-type: none"> Materials are synthesized by standard polymerization techniques enabling large scale production and scalability; 	<ul style="list-style-type: none"> Distribution of ligands at interface is difficult to assess 	[50-54, 56]
Alginate hydrogels	<ul style="list-style-type: none"> Could be used to fabricate complex 3D geometries (ex. tissue scaffolds) 		[57-62]
Alginate hydrogels with gold nanoparticles	<ul style="list-style-type: none"> Materials are commercially available enabling large scale production and scalability; Distribution of ligands at surface is easy to measure via standard imaging techniques 	<ul style="list-style-type: none"> The use of nanoparticles limits <i>in vivo</i> applications due to potential for nanoparticles to dislodge and result in toxicity 	[68]
PS-b-PEO block copolymer	<ul style="list-style-type: none"> Materials are commercially available; Distribution of ligands at surface is easy to measure via standard imaging techniques 	<ul style="list-style-type: none"> Surfaces are produced via spin casting, limiting sizes of surfaces that can be covered and limiting this technology to 2D interfaces 	[72-77]
Nanolithography techniques			

Nanoparticle arrays via micelle nanolithography	<ul style="list-style-type: none"> Enables exquisite control of local and global ligand density, distance between ligands within a nanoscale island, and distance between islands 	<ul style="list-style-type: none"> Limited <i>in vivo</i> applications due to potential toxicity of nanoparticles; Uses expensive and specialized equipment; 	[78-84, 86-95]
Nanoparticle arrays via nanoimprint lithography	<ul style="list-style-type: none"> Distribution of ligands at surface is easy to measure via standard imaging techniques 	<ul style="list-style-type: none"> Cannot be used for complex 3D shapes or to cover large surfaces areas Can only be fabricated on few background materials 	[96, 97]
Biotechnology techniques			
Protein chimeras	<ul style="list-style-type: none"> Enables precise control over number of ligands per nanoscale island; Can be used to surface functionalize complex 3D geometries 	<ul style="list-style-type: none"> Uses expensive and specialized equipment and molecular biology techniques; Distribution of ligands at interface is difficult to assess 	[98, 100]
Recombinant elastin-like protein	<ul style="list-style-type: none"> Can be used to fabricate complex 3D geometries 		[101]

Figure 1. The biophysics of integrin receptors: (A) Integrin receptors are non-covalently linked heterodimers that span the cell membrane. Externally, they bind with high specificity to polypeptide motifs in the external environment, while internally they link to the cell's cytoskeleton. (B) When bound to multivalent ligands, cells exhibit a full adhesion response that includes the formation of integrin-mediated adhesion complexes that contain structural proteins including talin and vinculin, adaptor proteins such as paxillin and tensin, and signalling molecules including focal adhesion kinase and Scr-family kinases.^[8, 11, 41] (C) When cells are adherent to biomaterials presenting monovalent ligands, focal adhesion formation, signalling events, and a variety of other cellular behaviors are impaired. (D) However, culturing cells on surfaces functionalized with multivalent ligands promotes the formation of adhesion complexes and exhibit a more biomimetic response including formation of focal adhesion and increased integrin-mediated signalling.

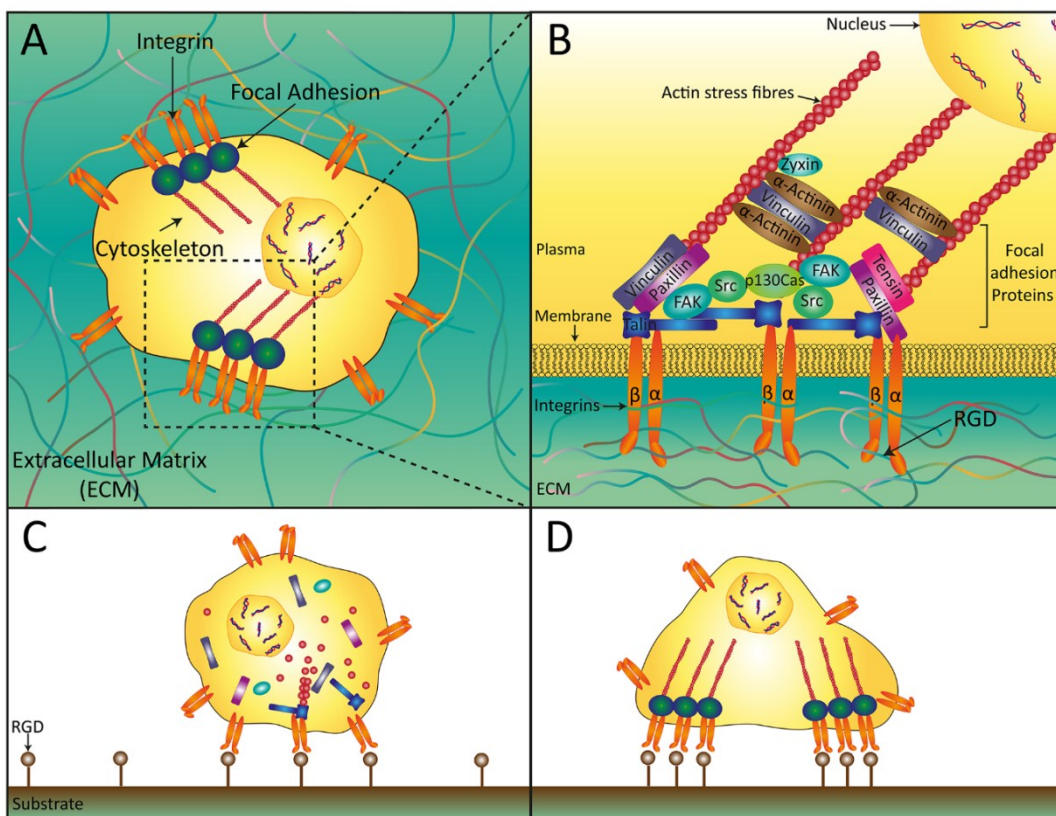


Figure 2. Historically, biomaterials have been biofunctionalized such that monovalent ligands (black dots) are randomly distributed across the interface (orange squares). Next generation biomaterials have been developed that provide biomaterials scientists and additional handle for innovation. Specifically, fabrication strategies have been designed to provide an experimenter with control over both the global ligand density and the nano-scale local ligand density. These advanced fabrication strategies enable researchers to tailor the total surface density of peptide, the valency of the ligands, the spacing of ligands within a cluster, and the spacing between ligand clusters.

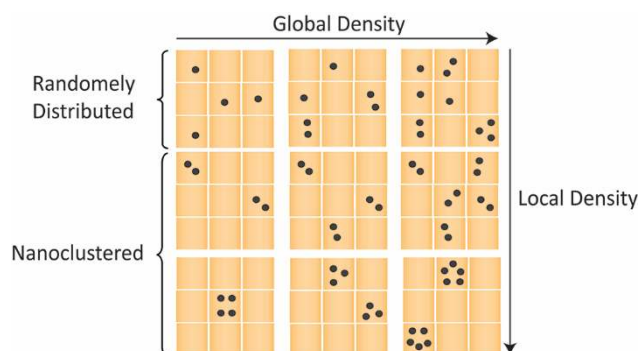


Figure 3. Several fabrication strategies have been developed to enable the development of materials with multivalent ligands. In this review, we differentiate these technique into three main categories: (1) Blending techniques where highly functional polymer molecules or nanoparticles are blended with non-functionalized polymer. Synthetic star polymers and comb polymers have been used along with naturally occurring alginate, and block copolymers. (2) Nanolithography techniques that enable surfaces to be functionalized with spatially patterned gold nanoparticles. These particles are then functionalized with ligand to enable precise control over ligand spacing. (3) Recombinant protein techniques where protein mimics are recombinantly expressed to display multivalent ligands.

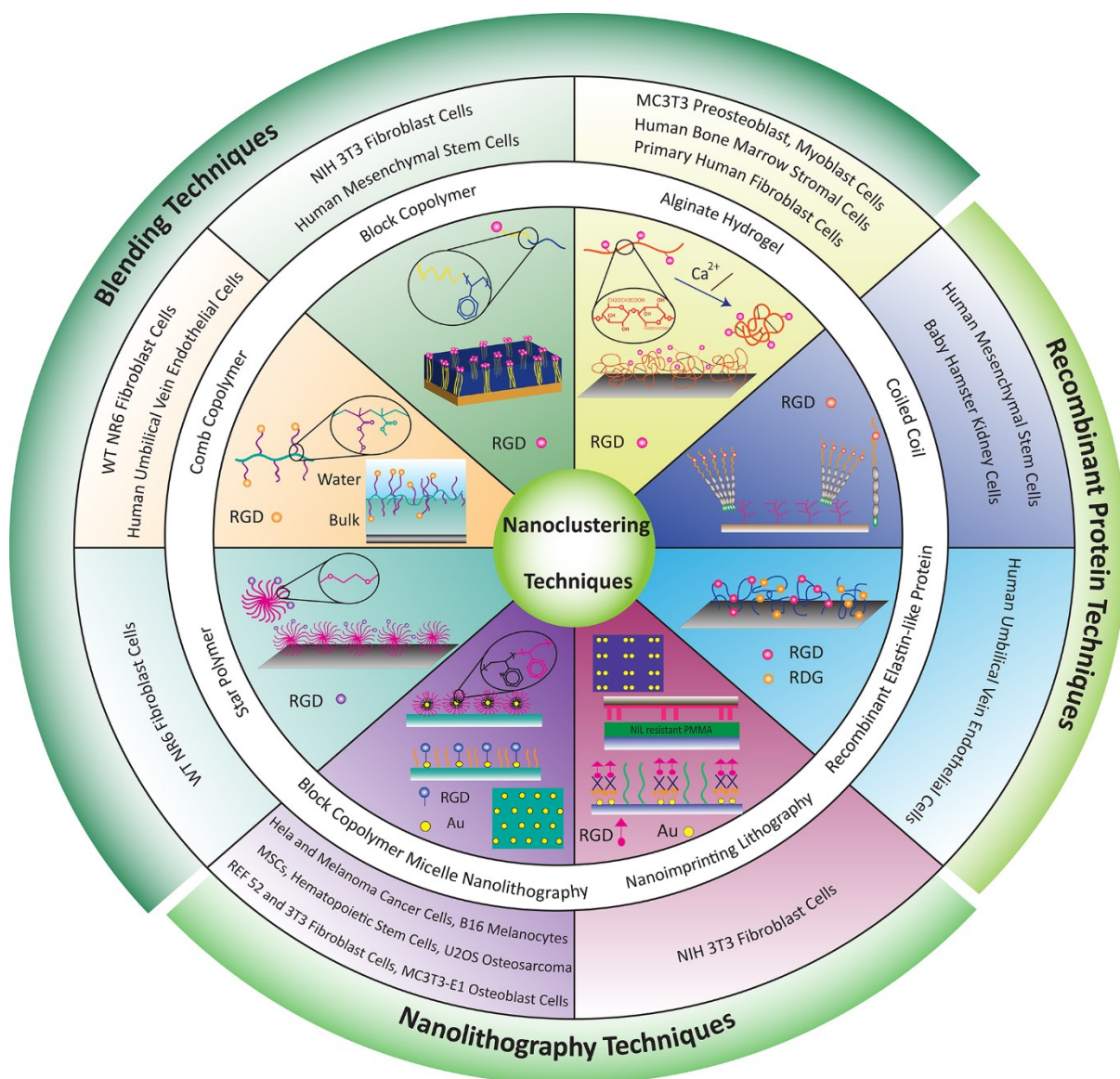


Figure 4. (A) The canonical method for biofunctionalized materials design is to randomly decorate a surface with ligand. (B) However, the blending strategy takes advantage of the nanometer size of individual polymer molecules or nanoparticles to generate multivalent ligands. The first report of this technology blended highly functionalized star polymers with non-functionalized star polymers.^[49] The degree of substitution of ligand onto the star determined the average valency of the ligand, the size of the star polymer defined the size of the island ligand, and the blending with non-functionalized star polymer determined the average spacing between islands of high ligand density.

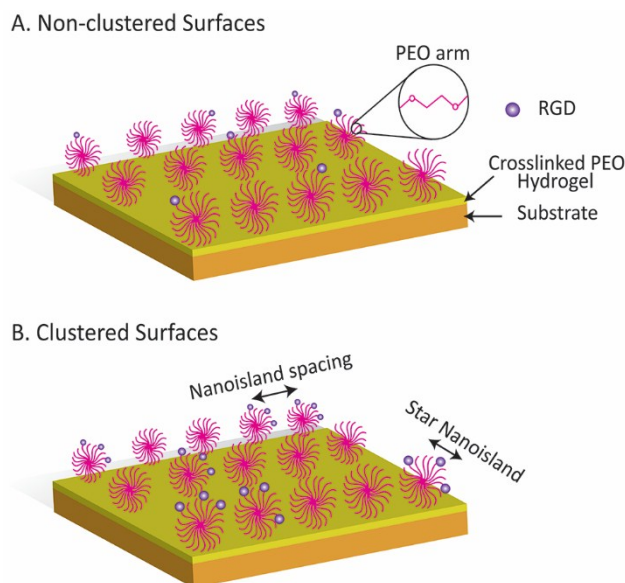


Figure 5. Comb polymers were developed that also enabled the fabrication of interfaces functionalized with multivalent ligands. These materials were polymerized as a random copolymer of methyl methacrylate and PEO-methacrylate. The methyl methacrylate results in a water insoluble material. When film cast, the polymer chains at the interface form a quasi-2D structure with the hydrophobic backbone of the polymer laying in the plane of the interface, and the hydrophilic pendant groups segregating into the aqueous phase and resulting in a non-fouling interface. When some of the polymer chains are highly functionalized with ligands, the size of their random coil structure governs the size of the multivalent ligands.

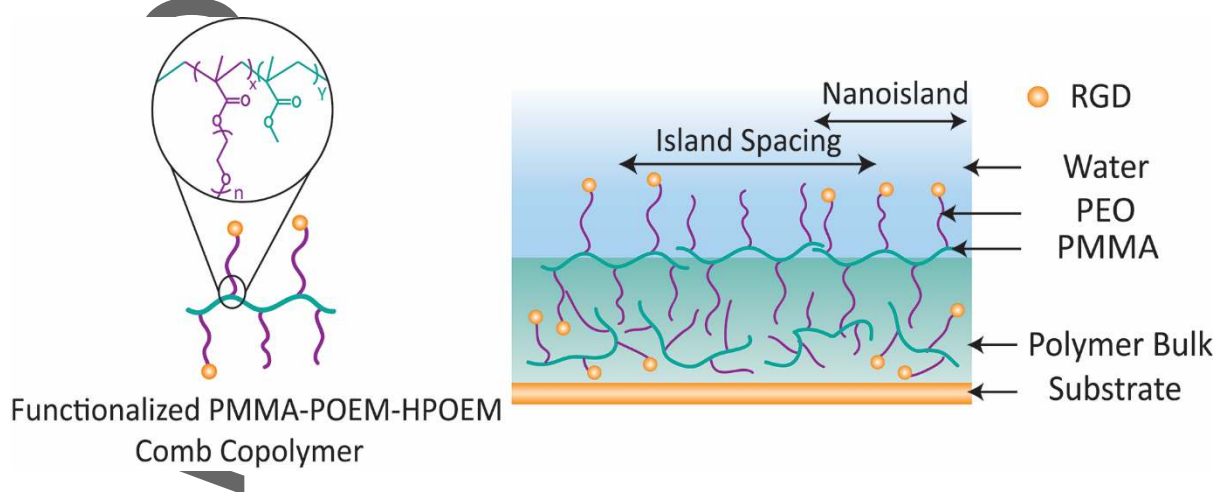


Figure 6. TEM analysis was used to confirm that films of the copolymer blends resulted in surfaces functionalized with multivalent ligands. After film casting, reactive groups that would be used to bind ligand were instead covalently linked to 1.4 nm gold nanoparticles. (A) These interfaces were then imaged with TEM to observe the distribution of nanoparticles at the surface. (B) Image analysis was used to predict the backbone of the individual polymer chains. Reproduced with permission.^[52] Copyright 2006, American Chemical Society.

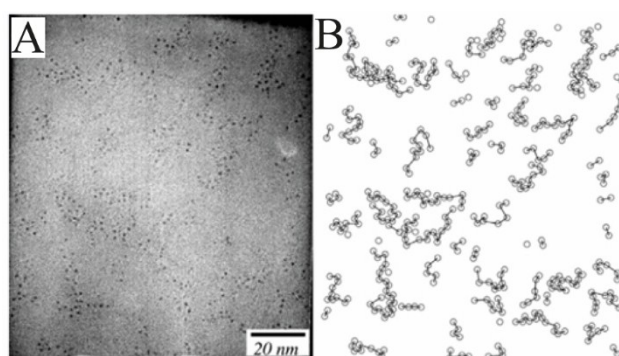


Figure 7. The peptides are often attached to the polymer via a flexible tether, a PEO pendant group in this case. It was identified that peptides attached to longer tethers of 14.3 nm enable more rapid cell spreading and focal adhesion formation compared to shorter tethers of 6.5 nm. The authors rationalized this observation by stating that the longer tethers provide the cells with a greater ability to rearrange the ligands at the interface.

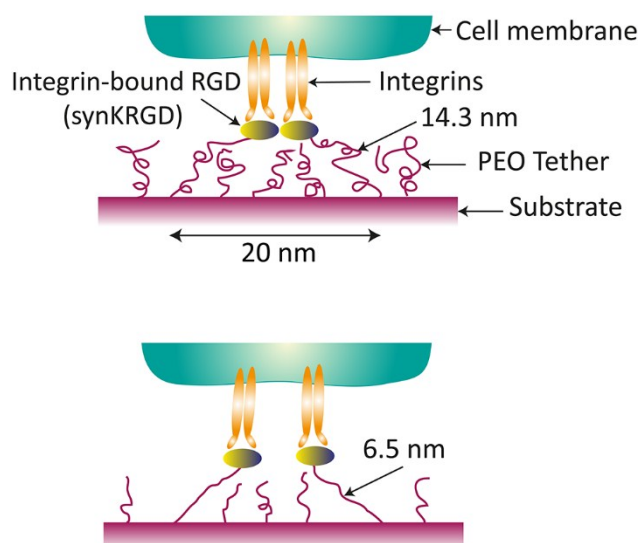


Figure 8. Alginate hydrogels functionalized with multivalent peptide ligands were also produced through a blending technique. First alginate polymers were highly functionalized with an RGD peptide, blended with non-functionalized polymer, and then crosslinked into the desired shape through the addition of calcium ions.

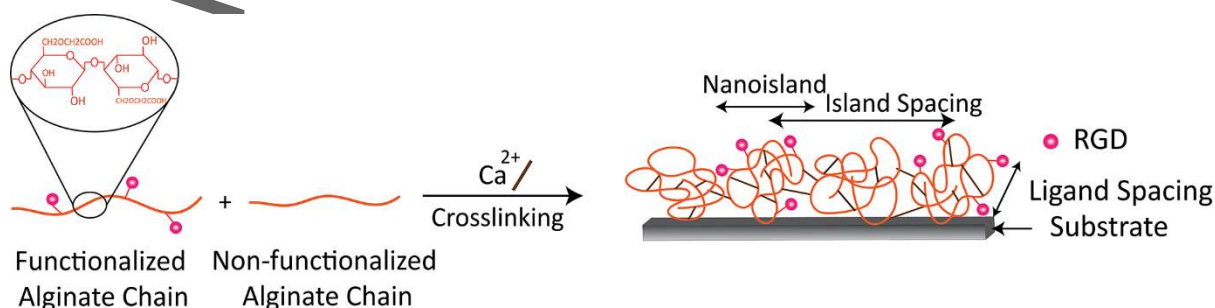


Figure 9. Researchers utilized diblock copolymers with hydrophobic blocks of polystyrene and hydrophilic blocks of PEO to produce nanopatterned surfaces through phase segregation. When these surfaces were spincoated, cylinders of hydrophilic PEO regions were dispersed in a hydrophobic background of polystyrene.^[72]

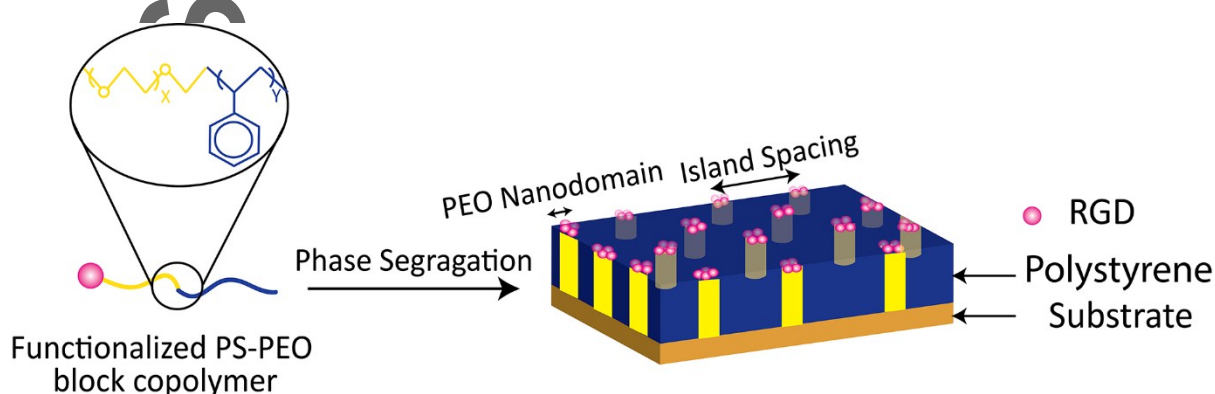


Figure 10. Block copolymer micelle nanolithography enables the fabrication of extended arrays of hexagonally packed gold nanoparticles. First, polystyrene-block-poly(2-vinyl pyridine) copolymers are synthesized through living polymerization. The polymers are then dissolved in toluene where they selfassemble to form micelles with polar cores. Tetrachloroaurate is then reduced with hydrazine resulting in the formation of gold nanoparticles within the core of the micelles. Substrates dip coated into this micelle solution are covered with a monolayer of hexagonally packed micelles. Plasma exposure removes the polymer components from the surface, resulting in a substrate covered with an extended array of gold nanoparticles with well-defined inter-particle spacing. The area between gold nanoparticles is then passivated with a non-fouling layer, and the gold nanoparticles are functionalized with cysteine-terminated polypeptides.

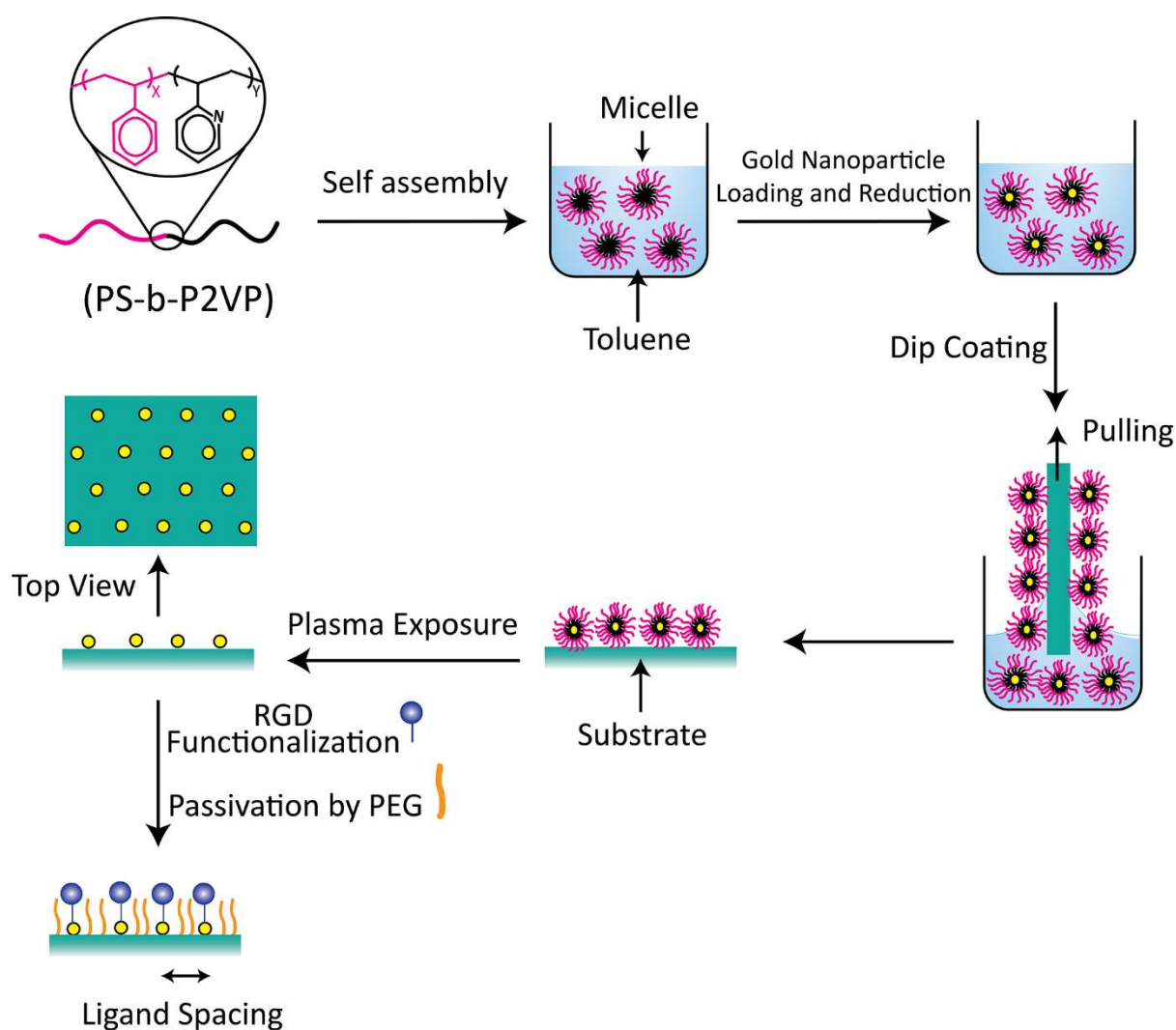


Figure 11. Glass surfaces covered with an extended array of quasi-hexagonally packed gold nanoparticles. Controlling the size of the polar and non-polar blocks within the copolymer enables control the nanoparticle size and the inter-particle spacing. The width of each image corresponds to 3 μm . Reproduced with permission.^[78] Copyright 2000, American Chemical Society.

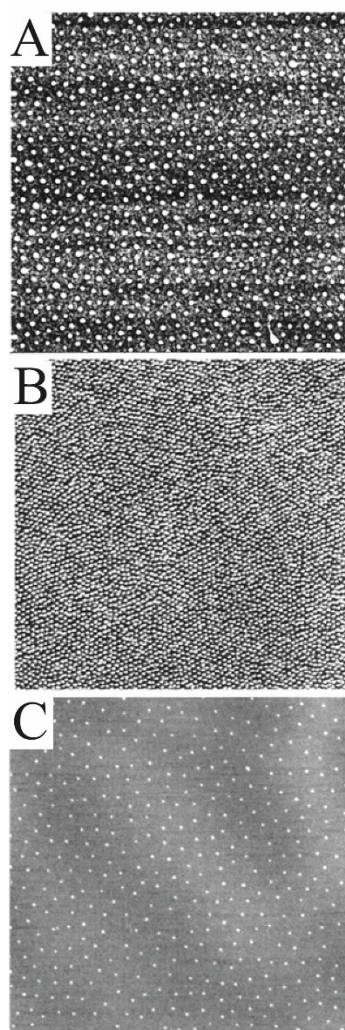


Figure 12. Rigid surfaces covered with extended arrays of gold nanoparticles were produced via block copolymer micelle nanolithography, as previously described (**Figure 10**). The gold nanoparticles are then reacted with a linker molecule, exposed to a PEO macromer solution, and crosslinked. During lift off of the PEO layer, the gold nanoparticles are also removed and result in a flexible substrate with an extended array of hexagonally packed gold nanoparticles on the surfaces. These gold nanoparticles are then functionalized through exposure to cysteine-terminated polypeptides.

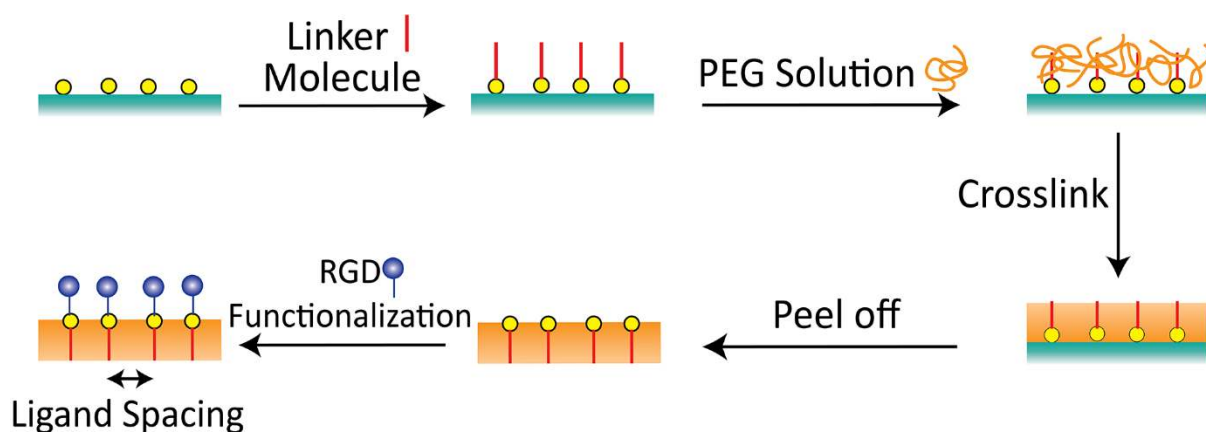


Figure 13. Rigid surfaces covered with extended arrays of micelles were produced via block copolymer micelle nanolithography, as previously described (**Figure 10**). The desired patterning of the surface was then defined through exposure to an e-beam to modify the micelles. Unmodified micelles and the nanoparticles they contain are removed through sonication in an organic solvent. The remaining micelles are removed through exposure to plasma to reveal surfaces covered with the desired patterning of nanoparticles.

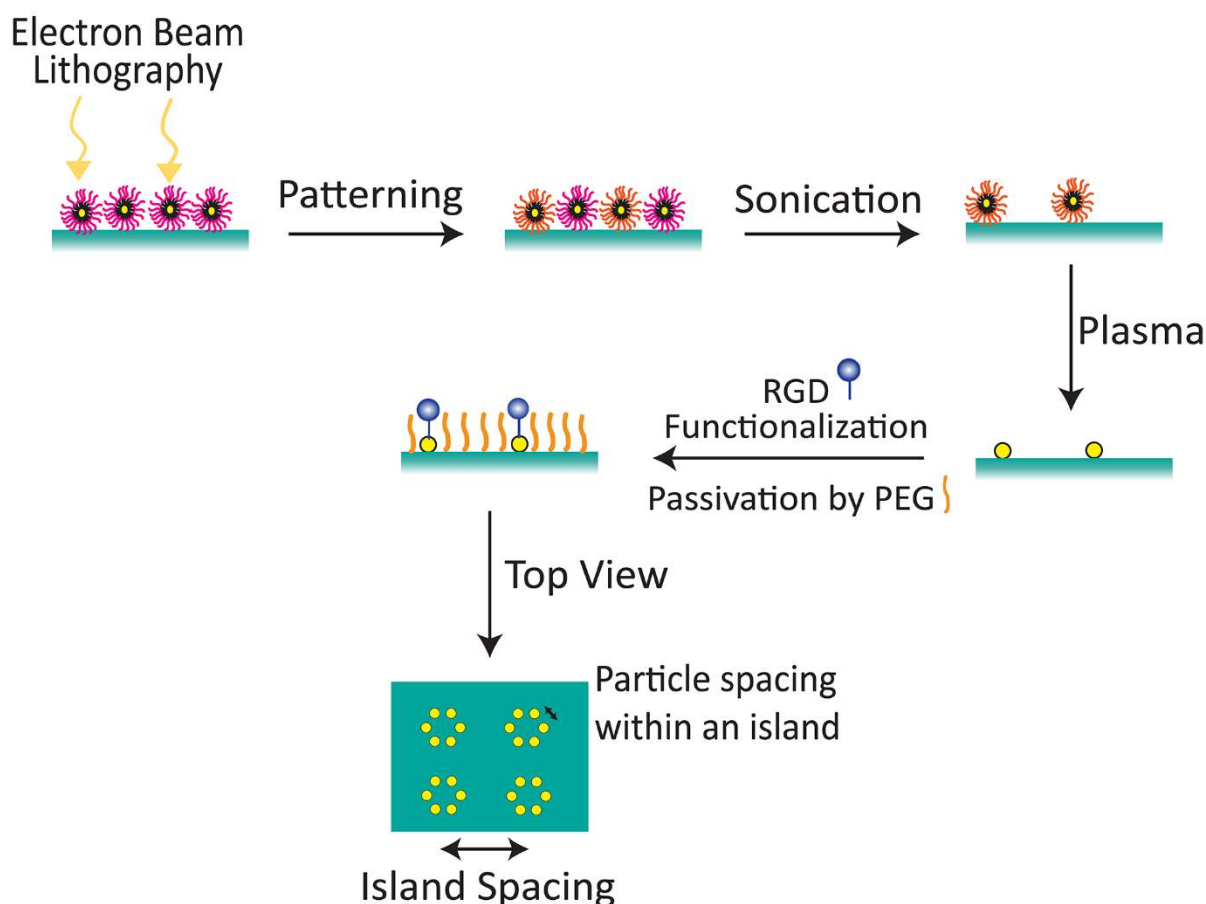
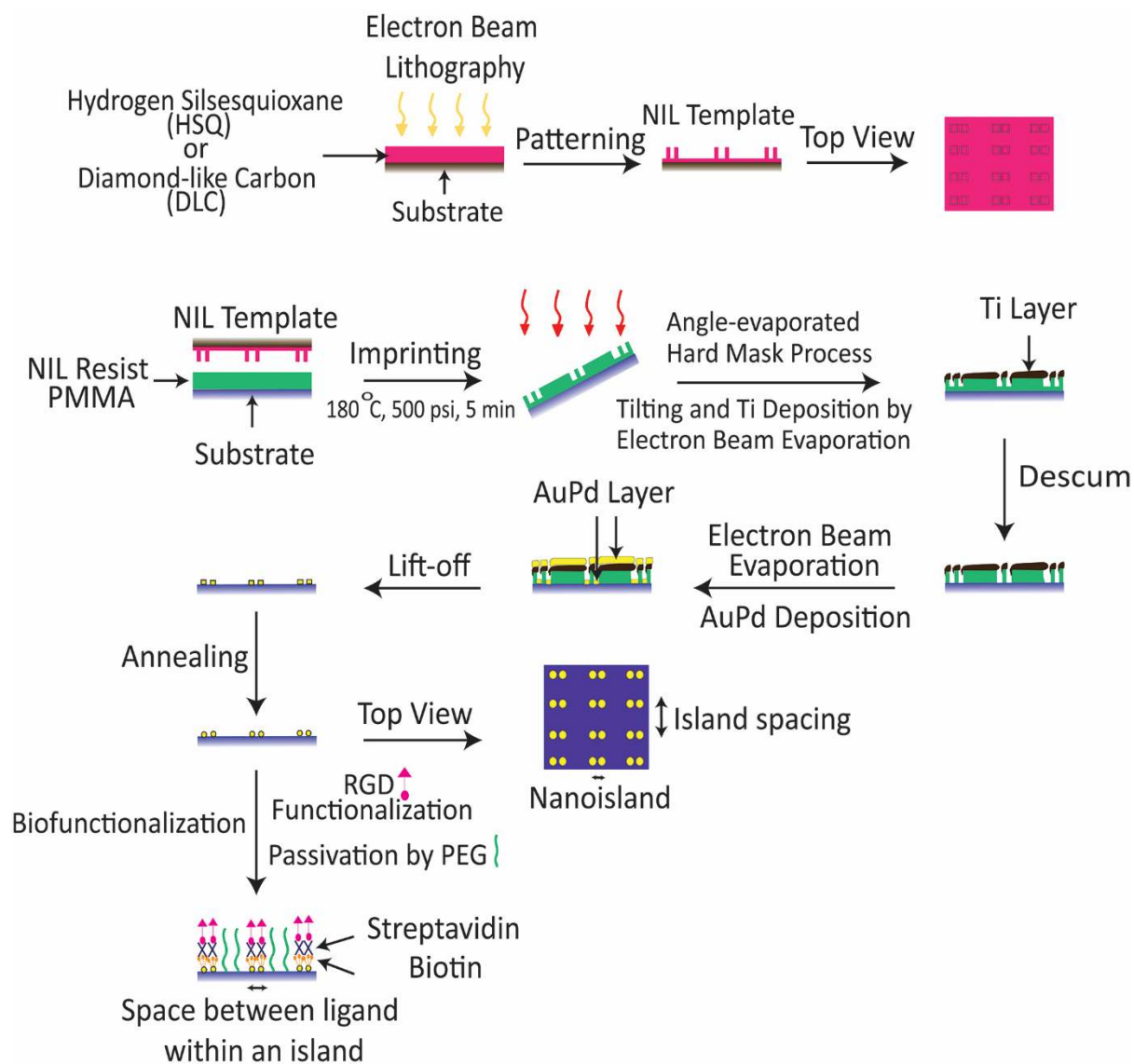


Figure 14. Nanoimprint lithography enables precise control over the spacing of individual ligands at the interface. NIL masks are made by patterning wafers coated with hydrogen silsesquioxane or diamond-like carbon using an e-beam. The pattern is transferred to a poly(methyl methacrylate) film, and titanium is deposited on the positive features through angled e-beam evaporation. After descumming, gold-palladium is deposited on the surface, lift off is performed, and the remaining gold-palladium regions are annealed to produce surfaces modified with gold-palladium nanoparticles with precise patterning. The surfaces are then passivated, and the nanoparticles are functionalized to add specific biological interactions.



Author

Figure 15. Multivalent protein chimeras produced by transfected *E. coli*. The chimera contains a polyhistidine tag to enable purification via chromatography, the FNIII₉₋₁₀ domain, a spacer group, a domain to enable selfassembly via coiled-coil interactions, and a terminal cysteine to enable surface functionalization through thiol chemistry.

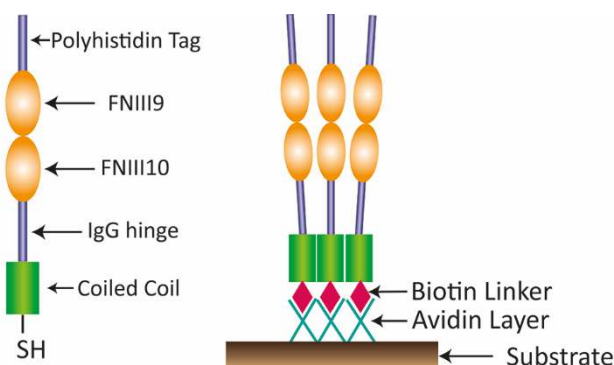


Figure 16. Multivalent protein chimeras containing the FNIII₇₋₁₀ domain were produced. The chimeras were then covalently linked to titanium surfaces that were pre-coated with a PEO layer.

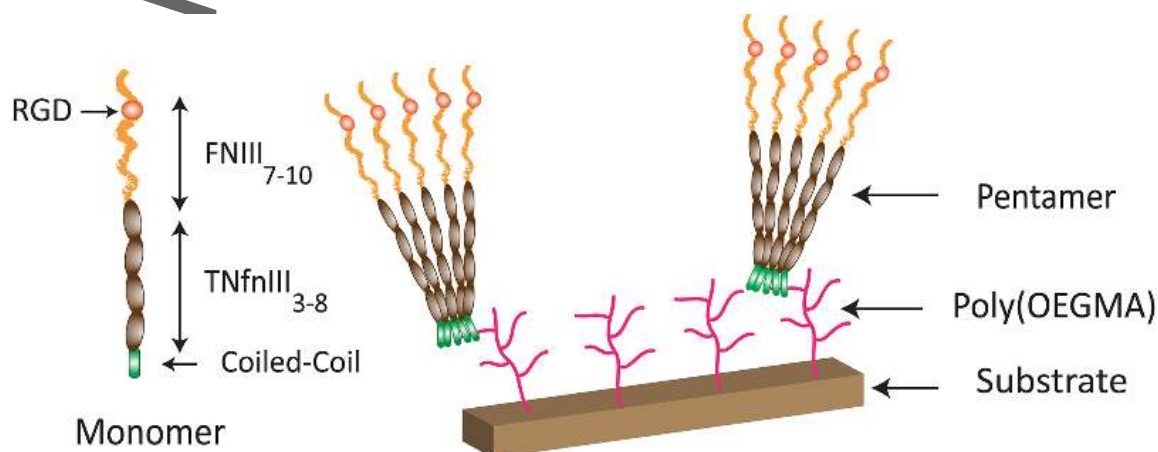
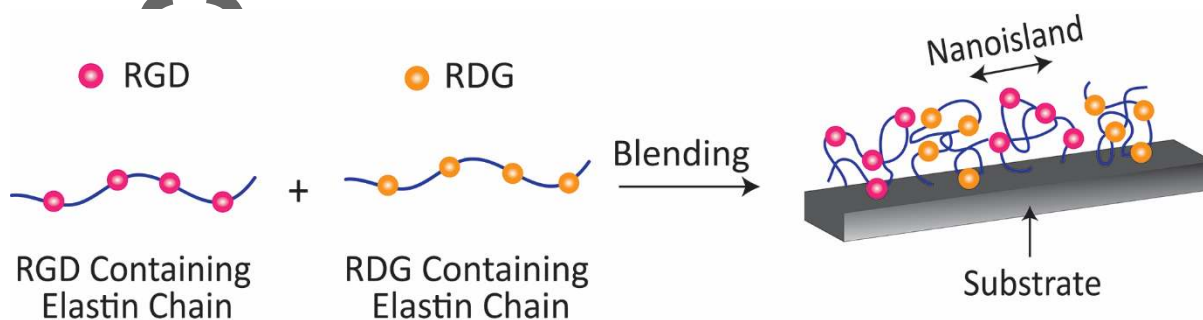


Figure 17. Recombinant elastin-like protein was produced that can be designed to contain cell adhesive (RGD) or non-adhesive (RDG) groups. The polymers could be blended in desired ratios in order to produce surfaces with controlled surface densities of the cell adhesive RGD ligand.

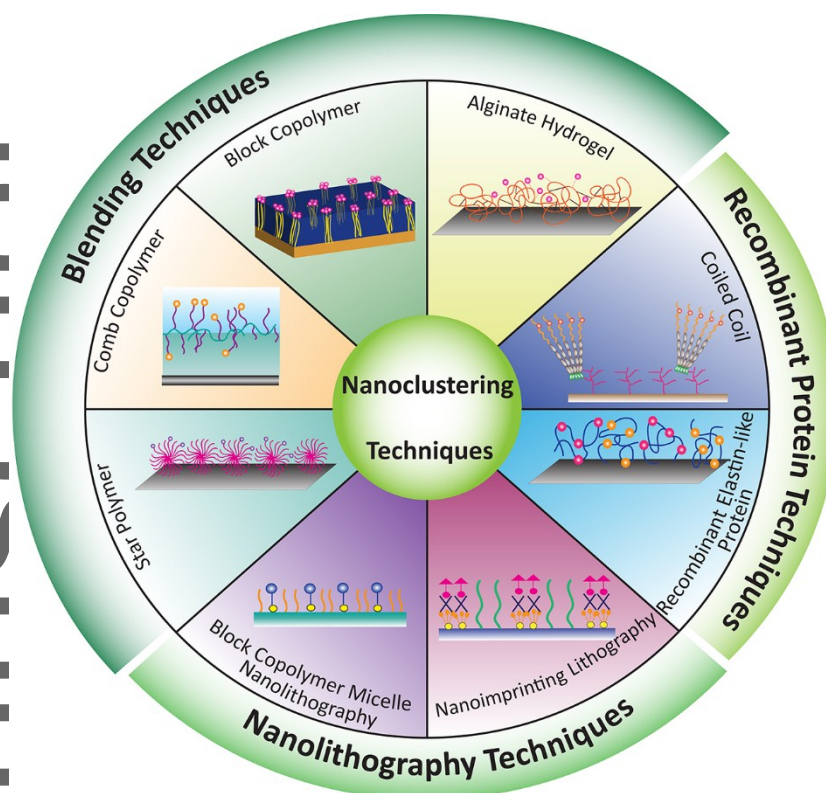


Title: Integrin Clustering Matters: A Review of Biomaterials Functionalized with Multivalent Integrin-Binding Ligands to Improve Cell Adhesion, Migration, Differentiation, Angiogenesis, and Biomedical Device Integration

Fatemeh Karimi, Andrea J O'Connor, Greg Qiao, Daniel E Heath**

The functionalization of biomaterial surfaces with nanoscale clusters of integrin-binding ligands has emerged as a powerful method of regulating the behaviour of adherent cells. However, the fabrication of such nano-structured materials is not a trivial. This review describes the techniques that have been developed to enable such materials to be fabricated; describes the improved biological properties that these material system can elicit, both *in vitro* and *in vivo*; and discusses future applications of these advanced healthcare materials.

Table of Content Figure



Fatemeh Karimi received her B.Sc. and M.Sc. degrees in Chemistry and Polymer Chemistry from the University of Tehran, Iran in 2010 and 2012, respectively. Her master degree focused on the investigation of structure-property relationship of biohybrid coacervates under the supervision of Assistant Professor Nader Taheri Qazvini. After a few years working in industry in Iran, she started her PhD in Chemical and Biomedical Engineering at the University of Melbourne in 2015 under the supervision of Dr. Daniel Heath, Professor Greg Qiao, and Associate Professor Andrea O' Connor. Her current research is focused on the design of advanced biomaterials to promote endothelialization for vascular graft applications.



Professor Greg Qiao received his Ph.D. at the University of Queensland in 1996. He joined the University of Melbourne in 1996 and became a full Professor in 2009. He was an Australian Research Council's professorial Future Fellow (2012-2015) and the Chair of Polymer Division of the RACI (2015-2016). He received ExxonMobil Award in 2015, RACI's Polymer Division Citation in 2011 and Freehills Award in 2010. He has published > 230 journal papers and is a co-inventor of > 20 patents. His key research interests are in polymeric architectures, new activation methods for RAFT, peptide polymers, tissue scaffolds, and gas membranes.



t

Daniel Heath completed his PhD in Chemical and Biomolecular Engineering at The Ohio State University in 2010 with Professor Stuart L. Cooper. He then undertook postdoctoral research at the Singapore-MIT Alliance for Research and Technology and MIT under the supervision of Professors Paula Hammond, Linda Griffith, and Mary Chan-Park. He began as a Lecturer at the University of Melbourne in 2014. Currently his lab focuses on the design of next generation biomaterials, both synthetic and extracellular matrix derived. His lab has a particular interest in blood contacting biomaterials such as vascular grafts and coronary artery stents as well as stem cell expansion.

Author Man



Minerva Access is the Institutional Repository of The University of Melbourne

Author/s:

Karimi, F;O'Connor, AJ;Qiao, GG;Heath, DE

Title:

Integrin Clustering Matters: A Review of Biomaterials Functionalized with Multivalent Integrin-Binding Ligands to Improve Cell Adhesion, Migration, Differentiation, Angiogenesis, and Biomedical Device Integration

Date:

2018-06-20

Citation:

Karimi, F., O'Connor, A. J., Qiao, G. G. & Heath, D. E. (2018). Integrin Clustering Matters: A Review of Biomaterials Functionalized with Multivalent Integrin-Binding Ligands to Improve Cell Adhesion, Migration, Differentiation, Angiogenesis, and Biomedical Device Integration. *ADVANCED HEALTHCARE MATERIALS*, 7 (12), <https://doi.org/10.1002/adhm.201701324>.

Persistent Link:

<http://hdl.handle.net/11343/283752>